



GRADUATE SCHOOL  
EAST TENNESSEE STATE UNIVERSITY

East Tennessee State University  
Digital Commons @ East  
Tennessee State University

---

Electronic Theses and Dissertations

Student Works


---

12-2020

## Prevention of Chronic Inflammation by Targeting Macrophage Integrin $\alpha$ Db2

Cady Forgey  
*East Tennessee State University*

Follow this and additional works at: <https://dc.etsu.edu/etd>

 Part of the [Molecular Biology Commons](#)

---

### Recommended Citation

Forgey, Cady, "Prevention of Chronic Inflammation by Targeting Macrophage Integrin  $\alpha$ Db2" (2020).  
*Electronic Theses and Dissertations*. Paper 3849. <https://dc.etsu.edu/etd/3849>

This Thesis - embargo is brought to you for free and open access by the Student Works at Digital Commons @ East Tennessee State University. It has been accepted for inclusion in Electronic Theses and Dissertations by an authorized administrator of Digital Commons @ East Tennessee State University. For more information, please contact [digilib@etsu.edu](mailto:digilib@etsu.edu).

Prevention of Chronic Inflammation by Targeting Macrophage Integrin  $\alpha_D\beta_2$

---

A thesis

presented to

the faculty of the Department of Biological Sciences

East Tennessee State University

In partial fulfillment

of the requirement for the degree

Master of Science in Biology

---

by

Cady Forgey

December 2020

---

Dr. Valentin Yakubenko, Chair

Dr. Jonathan Peterson

Dr. Patrick Bradshaw

Keywords: inflammation, macrophage, protein interaction, integrin, adhesion

## ABSTRACT

### Prevention of Chronic Inflammation by Targeting Macrophage Integrin $\alpha_D\beta_2$

by

Cady Forgey

Macrophage integrin  $\alpha_D\beta_2$  promotes macrophage retention and accumulation within inflamed tissue, a key event in development of chronic inflammation. Recently, the P5 peptide was identified as a specific inhibitor for integrin  $\alpha_D\beta_2$  interaction with 2-( $\omega$ -carboxyethyl) pyrrole (CEP), a ligand at inflammatory sites. This thesis aims to identify integrin  $\alpha_D$  I-domain amino acids involved in binding P5 peptide and likewise to CEP. We propose that non-conserved, basic amino acids of the integrin  $\alpha_D\beta_2$  I-domain are responsible for binding to P5 peptide and likewise to CEP. Eight amino acids were analyzed by generating six mutant  $\alpha_D$  I-domains: K180[A], R189[Q], K205[L], HHK223-225[NIT], K233[A], and K246[A]. Mutagenic constructs were created using PCR site-directed mutagenesis, then transformed into *E.coli* BL21 cells for IPTG-induced protein expression. Of the 6 mutant I-domains analyzed, amino acid K246 was critical in binding to P5 peptide and CEP through ForteBio Protein-Protein Assay, as well as to CEP by cell adhesion assay.

## ACKNOWLEDGMENTS

First, I would like to express my sincere appreciation for my committee chair and research mentor, Dr. Valentin Yakubenko Ph.D., for the opportunity to conduct this research and for his continuous support and direction throughout this thesis project. Without question, his expertise, intellect, patience, and passion for science made this research study possible and it was the greatest privilege to work under his guidance.

I would also like to thank my committee members, Dr. Jonathan Peterson Ph.D. and Dr. Patrick Bradshaw Ph.D., for their thoughtful insight and encouragement throughout my project which enhanced the outcome of this research.

Lastly, I would like to express my gratitude for my family as they inspire me to never stop pursuing my dreams.

## TABLE OF CONTENTS

	Page
ABSTRACT.....	2
ACKNOWLEDGEMENTS.....	3
LIST OF TABLES.....	7
LIST OF FIGURES.....	8
CHAPTER 1. INTRODUCTION.....	10
The Acute Inflammatory Response.....	11
The First Wave of Inflammation: Neutrophils.....	11
The Second Wave of Inflammation: Macrophages.....	12
Resolution of Inflammation.....	13
Chronic Inflammation.....	13
Role of Macrophages in Chronic Inflammation.....	14
The Integrin Family.....	16
Integrin Structure.....	17
$\alpha$ subunit.....	18
$\beta$ subunit.....	18
The B <sub>2</sub> Integrins.....	19
Integrin $\alpha_D\beta_2$ .....	20
Role of CEP- $\alpha_D\beta_2$ Interaction in Inflammation.....	21
P5 Peptide.....	22
Hypothesis.....	23
CHAPTER 2. EXPERIMENTAL PROCEDURES.....	24

Identification of Amino Acids for Mutation .....	24
NCBI Protein BLAST.....	24
3D Protein Structure Homology Modeling.....	24
Introduction of Mutation.....	24
Plasmid Construct.....	24
Generation of Mutagenic Primers.....	25
PCR-Site-Directed Mutagenesis.....	26
XL1-B Transformation.....	27
DNA Isolation.....	28
Protein Expression.....	29
BL21 Transformation.....	29
Cell Culture.....	29
Protein Expression with IPTG.....	29
Protein Isolation.....	30
Bacterial Cell Lysis.....	30
Ni-NTA Column Chromatography.....	30
Protein Dialysis.....	31
Protein Analysis.....	31
SDS PAGE.....	31
BCA Assay.....	32
Surface Plasmon Resonance Assay.....	32
Streptavidin Biosensor Assays.....	33
Amine Reactive (ARG2) Biosensor Assays.....	33

Cell Adhesion Assays.....	33
Cell Culture.....	34
Cell Transfection.....	34
Cell Sorting.....	34
Cell Adhesion.....	35
Experimental Design Flow Through.....	36
CHAPTER 3. RESULTS.....	37
Selection of $\alpha_D$ I domain Amino Acids for Analysis.....	37
Mutants K180[A] and R189[Q] are comparable to Wild-Type I-domain in P5 Peptide Binding.....	42
Mutants K205[L], HHK223-225[NIT], and K233[A] Demonstrated an Increase in P5 Peptide Binding Compared to the Wild-Type I-domain.....	47
Mutant K246 Demonstrated a Dramatic Reduction in Binding to both P5 Peptide and CEP Compared to Wild-Type.....	54
Comparison of Wild-Type and Mutant I-domain Binding P5 Peptide.....	57
$\alpha_D\beta_2$ -K246[A] Transfected HEK293 Cells Demonstrated a Significant Reduction in Binding to CEP.....	58
CHAPTER 4. DISCUSSION.....	61
REFERENCES.....	64
VITA.....	68

## LIST OF TABLES

Table 1. Primers Used for PCR Site Directed Mutagenesis.....	25
Table 2. PCR Sample Reaction Components.....	26
Table 3. QuikChange II Site-Directed Mutagenesis Cycling Conditions.....	27
Table 4. Process of Selecting $\alpha_D$ I-domain Amino Acids for Mutation.....	40
Table 5. Generation of Mutant Constructs.....	41



## LIST OF FIGURES

Figure 1. Inflammation.....	15
Figure 2. The Integrin Family.....	17
Figure 3. Integrin Structure.....	19
Figure 4. Comparative BLAST Analysis.....	38
Figure 5. Predicted Structure of the $\alpha_D$ I-domain.....	39
Figure 6. SDS-polyacrylamide gel electrophoresis (15%) for isolated WT and K180[A] I-domain protein.....	43
Figure 7. WT and Mutant K180 I-domain binding to P5.....	44
Figure 8. SDS-polyacrylamide gel electrophoresis (15%) for isolated WT and R189[Q] I-domain protein .....	45
Figure 9. WT and Mutant R189[Q] I-domain binding to P5.....	46
Figure 10. SDS-polyacrylamide gel electrophoresis (15%) for isolated WT and K205[L] I-domain protein.....	47
Figure 11. WT and Mutant K205[L] I-domain binding to P5.....	48
Figure 12. SDS-polyacrylamide gel electrophoresis (15%) for isolated WT and HHK223-225[NIT] I-domain protein.....	50
Figure 13. WT and Mutant HHK223-225[NIT] I-domain binding to P5.....	51
Figure 14. SDS-polyacrylamide gel electrophoresis (15%) for isolated WT and K233[A] I-domain protein.....	52
Figure 15. WT and Mutant K233[A] I-domain binding to P5.....	53
Figure 16: SDS-polyacrylamide gel electrophoresis (15%) for isolated WT and K246[A] I-domain protein. ....	54

Figure 17. WT and Mutant K246[A] I-domain binding to P5.....	55
Figure 18. WT and Mutant K246[A] I-domain binding to CEP. ....	56
Figure 19. Comparison of Mutant I-Domains Binding to P5 Peptide .....	57
Figure 20. WT and K246 Mutant $\alpha_D\beta_2$ -Transfected HEK293 Cells Adhering to CEP.....	59
Figure 21: WT and K246 Mutant $\alpha_D\beta_2$ -Transfected HEK293 Cells Adhering to Fibrinogen.....	60

## CHAPTER 1. INTRODUCTION

Inflammation is the fundamental mechanism used to defend host cells and repair host tissues after exposure to invading pathogens, harmful stimuli or physical injury. The inflammatory response describes a complex cascade of coordinated cellular events which function to first eliminate factors that interfere with homeostasis, followed by repairing the damage incurred by the surrounding tissue.<sup>1</sup> While inflammation is intended to be protective, failure to end an inflammatory response is often detrimental to host health. Unresolved inflammation leads to an accumulation of inflammatory cells, which over time has very damaging effects on host tissues and serves as the origin of chronic inflammatory disease.<sup>2,3</sup>

Diseases associated with chronic inflammation rank among the most significant causes of death worldwide and include cardiovascular disease, diabetes, cancer, arthritis and joint disease, allergies, and chronic respiratory diseases.<sup>4,5</sup> In May of 2017, the Rand Cooperation published a study which estimated that almost 60% of Americans live with at least one chronic inflammatory disease with the prevalence expected to steadily increase over the next 30 years.<sup>6</sup> Clearly, gaining a deeper understanding of the molecular mechanisms behind chronic inflammation and developing new methods to prevent and treat chronic inflammatory disease is imperative for human health.

A key event in the development of chronic inflammation is the accumulation and retention of pro-inflammatory macrophages within inflamed tissue. For this reason, targeting these pro-inflammatory macrophages has become an attractive avenue for developing new methods to prevent and treat chronic inflammatory reactions.<sup>7,8</sup> Expanding on several important findings by Yakubenko and his group, this thesis aims

to identify the specific amino acids of integrin  $\alpha_D\beta_2$  that participate in binding to the novel P5 peptide and likewise to 2-( $\omega$ -carboxyethyl) pyrrole, or CEP, a ligand at inflammatory sites. The introduction begins with a brief explanation of the acute inflammatory response, followed by a discussion of chronic inflammation, integrins, and previous findings by Yakubenko, his group, and others which led to the research project.

### *The Acute Inflammatory Response*

Acute inflammation serves as the first-line of defense following exposure to harmful stimuli or physical injury and is essential for maintaining host vitality.<sup>9</sup> An acute inflammatory response is initiated when pattern recognition receptors (PRRs) on the surface of resident immune cells recognize pathogen-associated molecular patterns (PAMPs) or damage-associated molecular patterns (DAMPs) present in the tissue.<sup>1</sup> Recognition of a PAMP or DAMP activates a resident immune cell and triggers the release of chemokines and several other inflammatory mediators. The release of these molecules alters the surface expression of nearby vascular endothelial cells, induces vasodilation, and increases blood flow and vascular permeability.<sup>10</sup>

### *The First Wave of Inflammation: Neutrophils*

When an inflammatory response is initiated, neutrophils are the first major cell type recruited to the site of inflammation. Changes in blood flow, vessel permeability and the molecular surface expression of cells lining the vessel wall allow circulating neutrophils to roll along the endothelium and enter the tissue through extravasation.<sup>11</sup> In the tissue, a chemokine gradient established by local cells and other chemoattractant molecules guide neutrophils towards the inflammatory site. Once at the site, neutrophils function in removal of pathogens by generating oxidative bursts, releasing granule

contents, phagocytosis, and through the formation of NETs.<sup>12</sup> Neutrophils have a major role in modulating the inflammatory response through releasing a variety of important inflammatory mediators. While neutrophils dominate the first phase of inflammation, we are now beginning to understand the importance of their roles which extend beyond this initial phase, including their formation of a close partnership with the macrophage which heavily influences the entire inflammatory response.<sup>13</sup>

### *The Second Wave of Inflammation: Macrophages*

Following the infiltration of neutrophils, monocyte-derived macrophages are the second major cell type to arrive at the site of inflammation. Circulating monocytes leave the bloodstream and transmigrate into the tissue by extravasation, where they differentiate into a macrophage.<sup>14</sup> Monocyte-derived macrophages are highly plastic cells of the immune system capable of altering their phenotypic expression based on a variety of signals and cues from the surrounding microenvironment.<sup>15</sup> This dynamic nature of macrophages allow them to play a major role in directing the inflammatory response, from phagocytic removal of insult and cell recruitment to later promoting healing and tissue regeneration during resolution phase of inflammation.

While a wide spectrum of possible phenotypes exist, macrophages are broadly characterized as M1-like or M2-like based on their mechanism of activation, molecular expression, and behavioral patterns. M1-like phenotypes are classically activated and are generally considered pro-inflammatory, while M2-like macrophages are alternatively activated and are generally considered anti-inflammatory.<sup>16</sup> M1-like macrophages are highly phagocytic and typically function at the inflammatory site to remove the stimulus, influence the behavior of nearby cells, and clear debris from the site. M1-like

macrophages stimulate inflammation by promoting recruitment of additional immune cells to the site and producing pro-inflammatory cytokines, chemokines and other inflammatory intermediates.<sup>17</sup>

### *Resolution of Inflammation*

As removal of the inflammatory stimulus is achieved, the macrophage population is believed to shift from an M1-like phenotype towards expression of an M2-like phenotype.<sup>18</sup> M2-like macrophages suppress the inflammatory response through releasing anti-inflammatory mediators, regulating behavior of other cells and promote healing and tissue regeneration.<sup>17</sup> Much remains unknown about these changes in macrophage phenotype expression, but the switch is highly regulated through many interconnected signals and pathways. This tight regulation is highly important as this transition in macrophage phenotype shifts the response from pro-inflammation to resolution of inflammation, repair and regeneration. Interestingly, neutrophil cell dying is among several factors shown to play a role in resolution of inflammation by influencing macrophages to express an M2 phenotype.<sup>13</sup> The anti-inflammatory M2-like macrophages direct the repair process and as the damaged tissue becomes restored, immune cells leave the site.<sup>19</sup> The acute inflammatory response is depicted in Figure 1A.

### *Chronic Inflammation*

By nature, the acute inflammatory response is intended to protect the host and repair damaged tissue. However, it is crucial that the inflammatory response be tightly regulated and that the resolution of inflammation is achieved.<sup>20</sup> Failure to resolve an inflammatory response leads to development of chronic inflammation, which contributes

significantly to the pathogenesis of many prevalent and devastating diseases.<sup>21</sup> While many pathways and cellular processes involved in initiating and maintaining an acute inflammatory response have become increasingly well-defined, much remains unknown about resolution of inflammation and the associated molecular pathways involved in development of chronic inflammation.<sup>22</sup> Unlike acute inflammation, chronic inflammation is a prolonged and maladaptive response which may originate due to underlying pathophysiology, exposures to certain substances, autoimmune disorders, oxidative stress, recurrent episodes of acute inflammation and in some cases, without apparent injury or disease.<sup>5</sup> Although there are several potential origins, a common key event in the development of chronic inflammation is the accumulation and retention of pro-inflammatory M1-like macrophages at the inflammatory site.

#### *Role of Macrophages in Chronic Inflammation*

Chronic inflammation occurs when leukocytes present at the site of inflammation are by some means unable to remove an inflammatory stimulus. As a result, additional leukocytes are continually recruited to the area in an attempt to overcome the insult. Over time, this leads to an accumulation of inflammatory cells, namely pro-inflammatory macrophages. As pro-inflammatory macrophages attempt to remove the stimulus using methods that result in collateral cell and tissue damage, their combined efforts have very damaging effects on the surrounding host tissue.<sup>22</sup> Over time, this leads to the formation of a chronic inflammatory lesion and the eventual development of a chronic inflammatory disease.<sup>23</sup> A schematic depicting acute and chronic inflammatory reactions is shown below in Figure 1B.

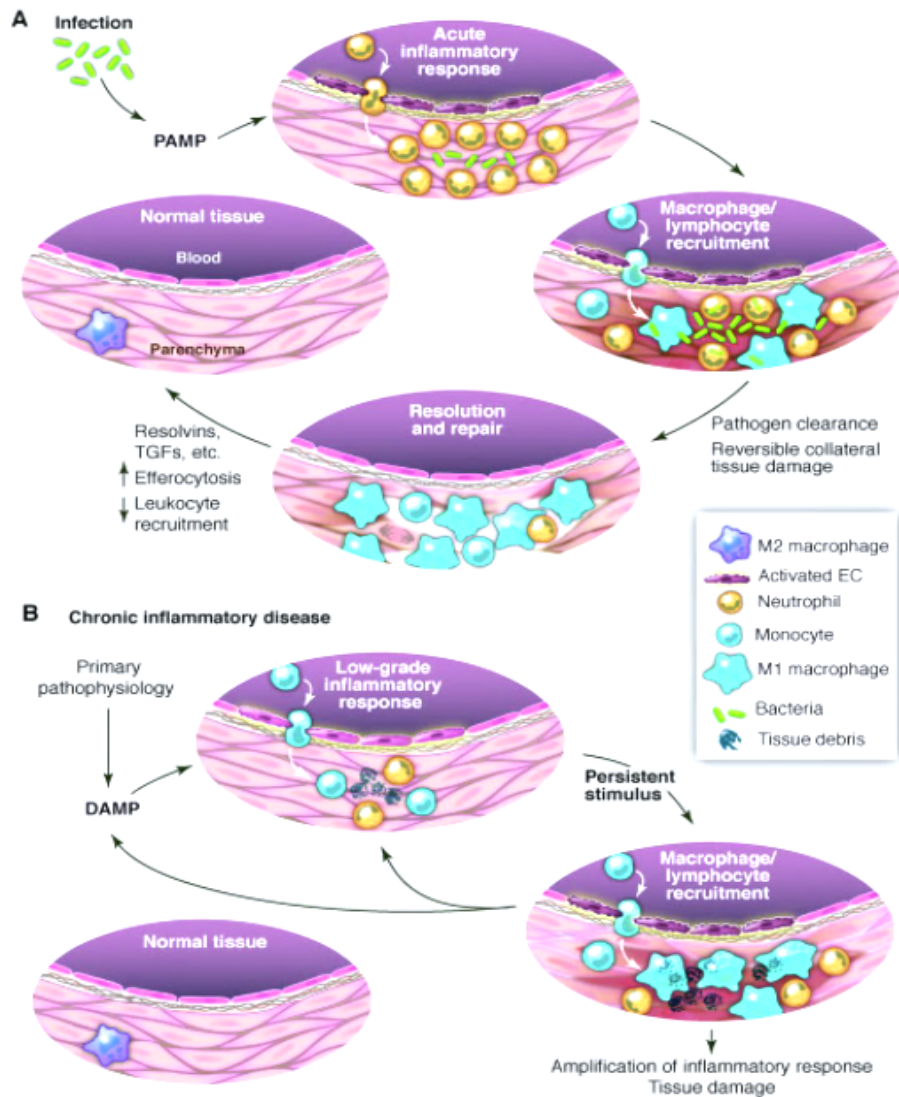


**Figure 1: Inflammation.** From Tabas I, Glass CK. Anti-inflammatory therapy in chronic disease: challenges and opportunities. *Science*. 2013;339(6116):166-172. Reprinted with permission from AAAS. **1A.** Progression of acute inflammation in response to a bacterial infection. Neutrophils are first to infiltrate the infected tissue, followed by the appearance of inflammatory monocyte-derived macrophages. After the pathogen is cleared, macrophages direct the immune response to resolution and repair stage until parenchyma is achieved. **1B.** Chronic inflammatory reactions occur when immune cells are unable to eradicate stimuli provoking an inflammatory response. The inflammatory



response is amplified due to the persistent presence of stimulus and resolution of inflammation is not achieved, resulting in host tissue damage.

As pro-inflammatory macrophages are the predominant cell population within these lesions and are also responsible for much of the damage sustained by chronic inflammatory reactions, inhibiting their ability to migrate and adhere to the site is an attractive method for prevention and treatment of chronic inflammatory reactions. During inflammation, the migration and adherence of monocytes and macrophages is largely mediated by the  $\beta_2$  integrins, an important subfamily of cell adhesion receptors which belong to the integrin family.

### *The Integrin Family*

Discovered in the late 1980's by Richard O. Hynes, the integrins are a large family of heterodimeric, glycoprotein adhesion receptors which span the cell membrane of virtually all nucleated metazoan cells.<sup>24, 25</sup> Collectively, the integrins carry out a variety of essential functions by allowing the cell to sense and respond to a dynamic extracellular environment. Serving as a physical link between the cell and its surroundings, integrins have direct roles in development, cell adhesion, cell migration, and cell-cell interactions.<sup>26</sup> Further, integrins are an integral part of several signal transduction pathways within the cell including those involved cell survival, transcriptional control, cell proliferation, cell motility, and organization of the internal cytoskeleton.<sup>27</sup> Currently, there are 24 members belonging to this essential family of adhesion receptors.

## Integrin Structure

Integrins are constructed from one  $\alpha$  and one  $\beta$  subunit held together by non-covalent interactions.<sup>28</sup> Consisting of a large globular head and two leg regions that insert into the plasma membrane, each integrin contains a large extracellular domain, a transmembrane domain, and a short cytoplasmic tail. The  $\alpha$  subunit forms one of the leg structures while the  $\beta$  subunit comprises the other. The large globular head is formed from the association of the  $\alpha$  and  $\beta$  subunits and contains the sites for ligand binding. In vertebrates, 24 integrin heterodimers are assembled from 18 different  $\alpha$  subunits and 8 different  $\beta$  subunits.<sup>29</sup> While the alpha and beta subunits do not show homology to each other, there are conserved regions and areas of homology within the group of alpha subunits and beta subunits themselves.<sup>27</sup> Each integrin heterodimer has a unique function and ligand-binding properties based upon their different individual subunit compositions. The 24 heterodimers of the integrin family are shown below in Figure 2.

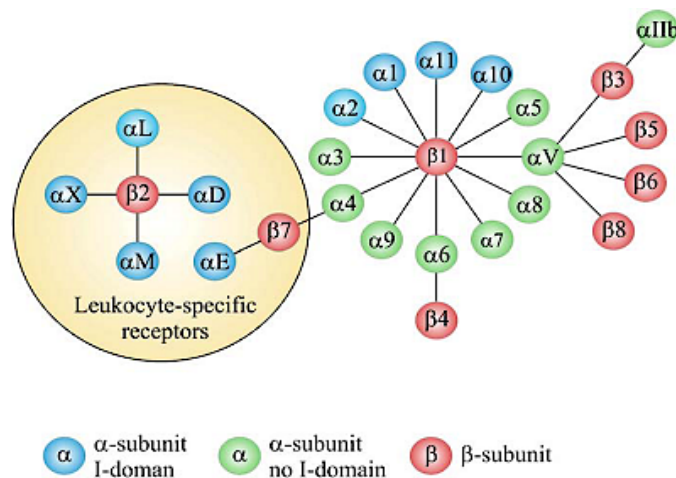


**Figure 2: The Integrin Family.** From Barczyk M., Carracedo S. & Gullberg D. *Integrins*. Cell Tissue Res. 2010; 339(269). Reprinted with permission from Elsevier. There are 24 heterodimers comprising the human family of integrins, each formed by the association of an  $\alpha$  and  $\beta$  subunit.

*α subunit.* Generally, the  $\alpha$  subunits are largely responsible for the ligand-specificity of each integrin. The extracellular portion of each  $\alpha$  subunit is composed of 4 domains: a thigh, a calf-1 domain, a calf-2 domain, and the seven-bladed  $\beta$ -propeller.<sup>30</sup> Together, the thigh, the calf-1 domain, and the calf-2 domain form a leg structure that supports the seven-bladed  $\beta$ -propeller of the integrin head. Of the 18  $\alpha$  subunits discovered thus far, 9 contain an additional I-domain which is inserted in-between blade 2 and blade 3 of the  $\beta$ -propeller.<sup>31</sup> The N-terminal I-domain consists of approximately 180 amino acids and is composed of 5  $\beta$ -sheets surrounded by 7  $\alpha$ -helices.<sup>31</sup> The I-domain is critical to ligand binding for integrins possessing this domain as it contains the metal ion-dependent adhesion site, or MIDAS. Located on the top face of the  $\alpha$  subunit I-domain, the ability of integrin to bind ligands is contingent on the binding of a divalent cation –  $Mg^{2+}$  or  $Mn^{2+}$  – at the MIDAS site.<sup>32</sup> Additionally, isolated integrin I-domains preserve the same ligand-binding abilities as the full length integrins.

*β subunit.* Each of the 8  $\beta$  subunits contain an I-like domain similar to those which are found in  $\alpha$  subunits.  $\beta$  subunits also contain a plexin/semaphoring/integrin (PSI) domain, a hybrid domain, four epidermal growth factor (EGF) repeats, and a membrane proximal  $\beta$  tail domain (bTD).<sup>33</sup> The image in Figure 3 below depicts the overall structure of an integrin heterodimer formed from the association of an  $\alpha$  and  $\beta$  subunit.

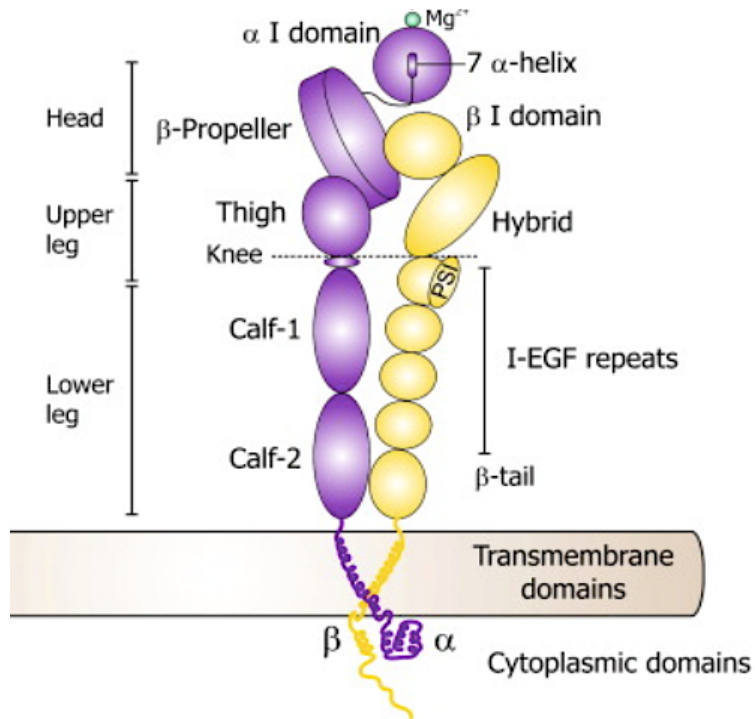


**Figure 3: Integrin Structure.** From Barczyk M., Carracedo S. & Gullberg D. Integrins. Cell Tissue Res. 2010; 339(269). Reprinted with permission from Elsevier. Integrins are composed of an  $\alpha$  and  $\beta$  subunit, held together by non-covalent interactions. Integrins have a large extracellular portion, short transmembrane domain, and short cytoplasmic tail.

### *The $\beta_2$ integrins*

There are four members within the  $\beta_2$  integrin subfamily:  $\alpha_L\beta_2$  (CD11a/CD18; LFA-1),  $\alpha_M\beta_2$  (CD11b/CD18, MAC-1),  $\alpha_X\beta_2$  (CD11c/CD18), and  $\alpha_D\beta_2$  (CD11d/CD18). Uniquely, the  $\beta_2$  integrins are only expressed on the surface of leukocytes and are not found on other cell types, hence their labeling as the leukointegrins.<sup>34</sup> While each different type of leukocyte expresses its own unique combination of integrins, the  $\beta_2$  integrins are the most abundantly expressed on their surfaces.<sup>35</sup> Leukocytes rely on the

$\beta_2$  integrins to carry out several essential mechanisms throughout the inflammatory response. These include cell interactions with endothelial cells during extravasion, interaction with the extracellular matrix within the tissue, cell adhesion, cell migration, phagocytosis, and the cell's ability to receive and respond to important inflammatory signals.<sup>35, 36</sup> Because of their selective expression on leukocytes and their heavy involvement throughout the inflammatory response, the  $\beta_2$  integrins have become very attractive therapeutic targets for a number of diseases. This thesis focuses on one particular member of the  $\beta_2$  integrin subfamily, integrin  $\alpha_D\beta_2$ , and its potential role in chronic inflammation.

*Integrin  $\alpha_D\beta_2$ .* Integrin  $\alpha_D\beta_2$  (CD11d/CD18) is the most recently discovered member of the  $\beta_2$  subfamily. While much remains unknown about this integrin, recent studies point to its key functions in inflammation, pathogen response, and tissue injury in experimental animals.<sup>37</sup> The crystal structure for integrin  $\alpha_D\beta_2$  currently remains unsolved, but the integrin does share significant homology in sequence with the other leukointegrins which are well-studied. The amino acid identities are very similar between  $\alpha_M$ ,  $\alpha_X$ , and  $\alpha_D$ , sharing 60-66% homology, while only 35% amino acid identify is shared with  $\alpha_L$ .<sup>38</sup> Current ligands identified for integrin  $\alpha_D\beta_2$  include ICAM-3, VCAM-1, fibrinogen, fibronectin, plasminogen, CYR6 and most recently CEP, a ligand found at sites of inflammation.<sup>39, 40</sup> Which types of human leukocytes express integrin  $\alpha_D\beta_2$  remains controversial but current research shows low to moderate expression on neutrophils and circulating monocytes, with upregulation on tissue macrophages – especially those within inflammatory lesions related to diseases such as atherogenesis and diabetes.

### *Role of CEP- $\alpha$ D $\beta$ 2 Interaction in Inflammation*

During inflammation, the generation of reactive oxygen species causes oxidative modifications to surrounding lipids and proteins. One such modification is 2-( $\omega$ -carboxyethyl) pyrole, abbreviated CEP, an adduct to proteins and phospholipids generated from oxidation of docosahexaenoic acid (DHA).<sup>41</sup> CEP generated *in-vivo* is biologically active and progressively accumulates under inflammatory conditions.<sup>42</sup> Interestingly, Yakubenko et. al recently proposed that during the first wave of inflammation, the oxidative insult generated by neutrophils significantly contributes to the formation of CEP and its addition onto surrounding components of the extracellular matrix.<sup>43</sup> After confirming CEP upregulation in inflammatory tissue in mice, they used CEP-blocking antibodies to demonstrate that early neutrophil invasion remained unaffected, while the subsequent appearance of macrophages was significantly reduced. They also showed that in the absence of neutrophils, the amount of CEP at the inflammatory site was significantly reduced. Importantly, they further demonstrated that CEP modifications to the extracellular matrix serves as a ligand for integrin  $\alpha$ D $\beta$ 2, which is dramatically upregulated on inflammatory macrophages.<sup>44</sup> As overexpression of this integrin causes excessive adhesion, this mechanism of integrin  $\alpha$ D $\beta$ 2 upregulation is believed to function as a brake signal which prevents further cell migration and thus promotes macrophage retention in inflamed tissue, especially during chronic inflammatory reactions where there is an abundance of CEP-decorated extracellular matrix proteins.<sup>45</sup>

Other macrophage receptors also recognize CEP for the purpose of binding and removing these CEP-tagged, damaged extracellular matrix components.<sup>42</sup> However,

blocking the interaction between CEP- $\alpha_D\beta_2$  is of high interest because of the unique expression pattern of  $\alpha_D\beta_2$  being low to moderate expression on circulating monocytes and significant upregulation on inflammatory macrophages.<sup>44</sup> Thus, creation of a specific CEP- $\alpha_D\beta_2$  inhibitor may have the potential to target and prevent macrophage accumulation and retention at sites of inflammation, which has very important clinical applications for prevention and treatment of chronic inflammatory diseases.

### *P5 Peptide*

These important discoveries were followed with another study by Cui et. al. which successfully identified a specific  $\alpha_D\beta_2$ -CEP inhibitor capable of preventing macrophage accumulation, named the P5 peptide.<sup>46</sup> The P5 peptide was identified through a specially designed peptide library, Biacore detected protein-protein interactions, and integrin transfected HEK 293 adhesion assays. The P5 peptide is 15 amino acids in length, with the amino acid sequence reading “GDAFDGDFGDDPSD.” The presence of 6 aspartic acid residues in the sequence confers a strong overall negative charge to the peptide. The P5 peptide was shown to specifically bind to integrin  $\alpha_D\beta_2$  and not to other leukointegrins such as  $\alpha_X\beta_2$  or  $\alpha_M\beta_2$ , which share very similar amino acid sequences. Using a thioglycollate-induced peritoneal model of inflammation, injection of cyclic P5 peptide reduced macrophage accumulation in WT mice by 3-fold, but had no effect in  $\alpha_D$ -deficient mice.<sup>46</sup> Additional experiments with the P5 peptide were very promising, as injection of cyclic P5 peptide into WT mice placed on a high fat diet prevented macrophage accumulation in an  $\alpha_D\beta_2$ -dependent manner in the adipose tissue.<sup>46</sup> Clearly, the P5 peptide prevents macrophage integrin  $\alpha_D\beta_2$ -mediated adhesion to CEP both *in-vivo* and *in-vitro*. These findings point to the critically important role of

integrin  $\alpha_D\beta_2$  in macrophage accumulation and retention during inflammation, and identify the P5 peptide as a potential inhibitor to prevent chronic inflammatory disease.

This thesis aims to identify the amino acids of integrin  $\alpha_D\beta_2$  which facilitate binding to the P5 peptide and similarly to CEP. Identification of these amino acids not only provides critical information for the development of a clinically relevant inhibitor of macrophage retention at the site of chronic inflammation, but also provides insight into the molecular interaction between integrin  $\alpha_D\beta_2$  and CEP.

### *Hypothesis*

We propose that non-conserved, basic amino acids of the integrin  $\alpha_D\beta_2$  located near the MIDAS site of the I-domain are responsible for binding to the P5 peptide and likewise to CEP.



## CHAPTER 2. EXPERIMENTAL PROCEDURES

### *Identification of Amino Acids for Mutation*

#### *NCBI Protein BLAST*

To identify potential  $\alpha_D$  I domain amino acids for mutation, a NCBI protein BLAST was performed which compared the human  $\alpha_D$  I domain amino acid sequence to that of the  $\alpha_M$  I domain. As the P5 peptide carries a negative charge and has been shown to not bind to  $\alpha_M\beta_2$ , non-homologous basic amino acid residues of the  $\alpha_D$  I domain were of interest.

#### *3D Protein Structure Homology Modeling*

To narrow the selection of potential amino acids for mutation, a previously generated computer model was used to determine the location of each selected amino acid of the  $\alpha_D$  I domain. Additionally, FirstGlance in Jmol software was used to identify the location for corresponding amino acids of  $\alpha_M$ . In each case, basic non-homologous amino acid residues near the  $\alpha_D$  I domain MIDAS site were of important interest as well as those contributing to an area of positive charge.

### *Introduction of Mutation*

#### *Plasmid Construct*

Recombinant human  $\alpha_D$  I domain DNA sequence encoding residues (D147-A331) was contained in pET-15b vector. The  $\alpha_D$  I-domain DNA sequence was inserted at the *NdeI* restriction site for transcription by bacterial T7 polymerase which recognizes the T7 promoter of the expression vector. Expression of the recombinant  $\alpha_D$  I domain sequence was under control of the lac operon and the vector provided resistance to ampicillin.

### Generation of Mutagenic Primers

Mutagenic primers were generated and analyzed using Oligo Primer Analysis Software version 6. The upper and lower primer sequences used for generating each mutation are shown below in Table 1.

**Table 1: Primers Used for PCR Site Directed Mutagenesis.** The mutagenic primer sequences for each mutation designed with Oligo Software.

Amino Acid	Upper Primer Sequence	Lower Primer Sequence
K180	5'-GCAGTACTCAAACCTCC TGGCGATCCACTTCACCTT CACC-3'	5'-GGTGAAGGTGAAGTGGAT CGCCAGGAGGTTTGAGTACT GC-3'
R189	5'- CCGTGAACGTCAGGCCTAGCA GTTGGACGATGGG-3'	5'-GGCTCGGGCTGGTCTGGA ATTGGGTGAAGG-3'
K205	5'-CCCATCGTCCAACCT GCTAGGCCTGACGTTT ACGG-3'	5'-CCGTGAACGTCAGGCCT AGCAGTTGGACGATGGG-3'
HHK 223-225	5'-GGTGACACAGCTA TTTAATATTACGAATGG GGCCCCGAAAAAG-3'	5'-CTTTTTTCGGGCCCCATT CGTAATATTAATAGCTGT GTCACC-3'
K233	5'- GCCCGAAAAAGTGCC GCGAAGATCCTCATTG TC-3'	5'-GACAATGAGGATCTTCG CGGCACTTTTTTCGGGC-3'
K246	5'-GATGGGCAGAAGTA CGCAGACCCCCTGGA ATACAG-3'	5'-CTGTATTCCAGGGGGTCT GCGTACTTCTGCCCATC-3'

The upper and lower mutagenic primers shown above in Table 1 were obtained from Integrated DNA Technologies Inc. (Coralville, Iowa).

### PCR Site-Directed Mutagenesis

PCR Site-Directed Mutagenesis was performed using the QuikChange II Site-Directed Mutagenesis Kit following the manufacturer's instructions (Agilent Technologies, Catalog # 200523). The kit components were thawed on ice and the sample reactions were prepared in a thin-walled PCR tube as shown below in Table 2.

**Table 2: PCR Sample Reaction Components.** The listed quantity or volume of each component was added to a thin walled PCR tube for generation of each mutagenic construct.

Component	Quantity/Volume
10x Reaction Buffer	5 $\mu$ L
dsDNA Template	50 ng
Upper Mutagenic Oligonucleotide Primer	125 ng
Lower Mutagenic Oligonucleotide Primer	125 ng
dNTP Mix	1 $\mu$ L
ddH <sub>2</sub> O	to final volume of 50 $\mu$ L

After each of the sample reaction components were placed in the tube and gently mixed, 1  $\mu$ L of *PfuUltra* HF DNA polymerase provided with the kit was added to the reaction. The sample reaction was then placed in a thermal cycler (BioRad T100) and cycled through the following conditions shown in Table 3 below as recommended by the manufacturer.

**Table 3: QuikChange II Site-Directed Mutagenesis Cycling Conditions.** Each mutagenic construct created by PCR Site-Directed Mutagenesis was cycled through the listed conditions.

Segment	Number of Cycles	Temperature	Time
1	1	95°C	30 seconds
2	18	95°C	30 seconds
		55°C	1 minute
		68°C	5 minutes 30 seconds
3	1	4°C	∞

Following the temperature cycling, the sample reaction was placed on ice for 2 minutes to cool. To digest unmutated template DNA, 1 uL of *Dpn* I restriction enzyme was added directly to the sample and gently mixed. The reaction was incubated at 37°C for 1 hour before transformation of XL1-B cells.

#### *XL1-B Transformation*

XL1-B Supercompetent cells were transformed following the manufacturer's protocol (Agilent Technologies, Catalog # 930236). The cells were first thawed on ice for 30 minutes, followed by the addition of 1 uL of *Dpn* I-treated DNA from the PCR sample reaction. The transformation reaction was gently swirled and placed on ice for 30 minutes. The transformation reaction was then heat-pulsed for 45 seconds in a 42°C water bath and immediately placed on ice for 2 minutes. Preheated 42°C SOC medium (Thermo Scientific, Catalog # 15544034) was added to the reaction, followed by an incubation at 37°C for 1 hour with shaking at 225 rpm. After incubation, the transformation reaction was plated on LB agar containing 100 ug/mL ampicillin and

placed in a 37°C incubator overnight. The next day, single colonies were selected from the transformation plate, individually placed in 3 mL TB media containing 100 ug/mL ampicillin, and cultured overnight.

#### *DNA Isolation*

DNA was isolated from the XL1-B cell culture using the QIAprep Spin Miniprep Kit by Qiagen (Catalog # 27104). Following the manufacturer's instructions, 3 mL of bacterial cell culture was placed in a table-top microcentrifuge (Sorvall Legend Micro 21R Refrigerated Centrifuge, Catalog # 75002447) and spun at 8000 rpm for 3 minutes at room temperature. The pelleted bacterial cells were resuspended in 250 uL Buffer P1. Buffer P2 was then added, the sample was mixed, and Buffer N3 was added. The sample was immediately mixed by inverting the tube and placed in the microcentrifuge for 10 minutes at 13,000 rpm. The supernatant was collected and transferred to a QIAprep 2.0 spin column and centrifuged for 1 minute. Buffer PE was added to the spin column and then centrifuged for 1 minute. All buffers mentioned were provided with the kit. To move residual wash buffer, the spin column was centrifuged again for another minute. To elute the DNA, the spin column was transferred to a clean microcentrifuge tube and 50 uL of warm water was added to the center of the spin column. The column was allowed to stand for 1 minute and then centrifuged for one minute. DNA concentration was determined by spectrometer (Synergy H1 Hybrid Multi-Mode Microplate Reader, BioTek Instruments).

## *Protein Expression*

### *BL21 Transformation*

BL21(DE3) competent cells were transformed according to manufacturer's instructions (Agilent Technologies, Catalog # 200133). Competent cells were thawed on ice for 30 minutes. Next, 50 ng of DNA containing the desired mutation was added to the cells and incubated on ice for 30 minutes. After incubation, the transformation reaction was heat-pulsed for 45 seconds in a 42°C water bath. The reaction was placed on ice for 2 minutes, followed by addition of preheated 42°C SOC medium to the cells. The cells were incubated at 37°C for 1 hour with shaking at 225 rpm. Following incubation, cells were plated on LB agar containing 100 ug/mL ampicillin and incubated at 37°C overnight.

### *Cell Culture*

A single colony taken from the transformation plate was placed in 3mL TB media containing 100 ug/mL ampicillin. The cells were cultured for 7-9 hours at 37°C with shaking at 225 rpm. Next, 200 uL of the culture was transferred to 200 mL TB media + 100 ug/mL ampicillin and grown overnight. The next morning, the 200 uL of culture was brought up to 2 liters by addition of 1.8 L of fresh TB media + 100 ug/mL ampicillin. The 2 liters were split evenly between 4 flasks and cultured at 37°C with shaking for 2-2.5 hours until reaching an optical density of 1.

### *Protein Expression with IPTG*

Recombinant protein expression was induced by addition of isopropyl  $\beta$ -D-thiogalactopyranoside (IPTG) to the bacterial culture for a final concentration of 1mM. Cells were incubated at 37°C with shaking for another 4 hours.

## *Protein Isolation*

### *Bacterial Cell Lysis*

After induction of protein expression, bacterial cell cultures were centrifuged at 6,000 RPM (3951 RCF) and 4°C for 20 minutes. The supernatant was discarded and the bacterial cell pellet was lysed by resuspension in 1% Triton + PBS. The bacterial cell lysate was frozen overnight at -80°C. The next day, the bacterial lysate was thawed in a 37°C water bath. To destroy chromatin, lysate was placed on ice and sonicated twice for 2 minute intervals. After sonification, the lysate was centrifuged at 15,000 rpm (16556 RCF) for 30 minutes at 4°C. The supernatant containing protein was collected and the pellet discarded.

### *Ni-NTA Column Chromatography*

Proteins were isolated using Ni-NTA Column Chromatography. To stabilize the protein and block non-specific binding, imidazole and NaCl were added to the supernatant for a final concentration of 10mM imidazole and 500mM NaCl. The supernatant containing protein was then incubated with HisPur Ni-NTA Superflow Agarose (Thermo Scientific, Prod# 25214) at 4°C for 1 hour with gentle rocking. After incubation, the sample was placed in a centrifuge and spun at 4°C and 1200 rpm for 10 minutes (Heraeus™ Multifuge™ X3 Centrifuge, Thermo Scientific). The bottom layer containing Ni-NTA agarose bound to protein was collected using a pipette and transferred to a Poly-Prep Chromatography Column (Bio-Rad Laboratories, Catalog #731-1550) for isolation. Once the Ni-NTA agarose bound to protein was loaded into the column, the column was washed with 40mL of 20mM imidazole or until the eluent had reached an optical density of less than 0.1. This was followed by washing with 20 mL of

60mM imidazole or until the eluent had reached an optical density of less than 0.05. The final wash step was with 20 mL of 80mM imidazole or until the eluent reached an optical density of less than 0.01. After completing the washing steps, the protein was eluted with 5 mL 250mM imidazole into 5 separate samples of 1mL each. The pre-dialysis concentration of protein in each sample was determined by spectrometer (Synergy H1 Hybrid Multi-Mode Microplate Reader, BioTek Instruments).

### *Protein Dialysis*

Isolated protein samples were combined and placed in dialysis tubing by Fisherbrand (# 21-152-10). For the first phase of dialysis, the proteins were placed in 500mL PBS + 1M NaCl for 30 minutes at 4°C with gentle stirring. Next, the proteins were switched into 500mL PBS + 500mM NaCl at 4°C with gentle stirring and left overnight. The next morning, the proteins were placed into 500mL 20mM Hepes + 150mM NaCl for 4 hours at 4°C with gentle stirring. The protein was collected and post-dialysis protein concentration was checked with spectrometer (Synergy H1 Hybrid Multi-Mode Microplate Reader, BioTek Instruments).

### *Protein Analysis*

#### *SDS-PAGE*

The amount and purity of protein was visualized by performing SDS-PAGE. For each sample, 6 uL of 5x SDS loading buffer was added a 24 uL sample of the protein. The protein samples were heated for 5 minutes at 100°C. The protein ladder (Precision Plus Protein™ Dual Color Standards, 500 µl #1610374, BioRad) was added to the first well of a 15% polyacrylamide gel, followed by loading of each protein sample into subsequent wells. After running the gel and separation of protein, the gel was washed



with a 10% acetic acid, 50% methanol, and 40% water solution. The gel was stained with a 90% water, 10% acetic acid solution containing Coomassie blue R250, Coomassie blue G250, and amido black.

#### *BCA Assay*

Protein concentrations were also measured using the Pierce BCA Protein Assay Kit (Thermo Scientific, Product # 23227) following the manufacturer's instructions. Standards ranging from 0 ug/mL to 2000 ug/mL were prepared from Bovine Serum Albumin provided with the kit and diluted with buffer containing 20mM HEPES and 150mM NaCl. Then, 25 uL of each standard and protein sample were added to individual wells of a 96 well plate (Immulon, 2HB). After adding standards and samples into the plate, 200 uL of working reagent provided by the kit was added to each well containing a standard or samples. The plate was incubated at 37°C for 45 minutes. Following incubation, the plate was allowed to cool and absorbance at 562 nm was measured for each standard and sample using the Synergy H1 Hybrid Multi-Mode Microplate Reader from BioTek Instruments. The absorbance and known concentrations of each standard were used to generate a standard curve on Microsoft Excel. The concentration of each sample protein was calculated using the generated standard curve.

#### *Surface Plasmon Resonance Assays*

The binding abilities of wild-type  $\alpha_D$  I domain protein and mutant  $\alpha_D$  I domain protein to various ligands were assessed through surface plasmon resonance assays using the ForteBio K2 Octet system.

### *Streptavidin Biosensor Assays*

To test protein binding to the P5 peptide, biotinylated P5 peptide was immobilized onto an activated streptavidin biosensor chip from ForteBio. Preparation of the streptavidin chip and recording of sensorgrams were carried out according to manufacturer's instructions. Each streptavidin biosensor was soaked in buffer containing 20mM Hepes, 150mM NaCl and 1mM CaCl<sub>2</sub> to remove the protective surface. Proteins to be assayed were diluted to desired concentrations in buffer containing 20mM Hepes, 150mM NaCl, 1mM CaCl<sub>2</sub>, 1mM MgCl<sub>2</sub> and 0.02% Tween.

### *Amine Reactive (ARG2) Biosensor Assays*

Amine Reactive (ARG2) ForteBio biosensor chips were used to test protein interaction with CEP. The protective surface of the ARG2 biosensor was removed by soaking in buffer containing 20mM Hepes, 150mM NaCl and 1mM CaCl<sub>2</sub>. The ARG2 biosensors were activated with N-hydroxysulfosuccinimide (s-NHS) and 1-Ethyl-3-(3-(dimethylamino)propyl)carbodiimide (EDC). Ligands to be tested were placed in Sodium Acetate solution adjusted to pH 5 and immobilized onto the activated biosensor surface. Unreacted sites on the biosensor surface were quenched with 1M Ethanolamine. Proteins were assayed in buffer containing 20mM Hepes, 150mM NaCl, 1mM CaCl<sub>2</sub>, 1mM MgCl<sub>2</sub> and 0.02% Tween.

### *Cell Adhesion Assays*

Mutant I-domain which showed a decrease in binding to P5 peptide was selected for further analysis by cell adhesion assay.

### *Cell Culture*

The  $\alpha_D\beta_2$ -transfected Human embryonic kidney 293 cells were maintained in DMEM-F12 (BioWhittaker, Walkersville, MD) supplemented with 10% FBS, 2 mM glutamine, 15 mM HEPES, 0.1 mg/ml streptomycin and 0.1 unit/ml penicillin.

### *Cell Transfection*

Site-directed mutagenesis of the  $\alpha_D$  subunit was performed using the QuickChange™ Mutagenesis Kit. The pcDNA3.1/Neo(-) construct containing DNA encoding the full-length  $\alpha_D$  subunit was modified by site-directed mutagenesis using two mutagenic primers containing the desired mutation. Cells were stably transfected with pcDNA3.1 plasmids with inserted  $\beta_2$  and wild-type or mutant  $\alpha_D$  using Lipofectamine™ 2000 reagent (Invitrogen, San Diego, CA). After 48 h at 37°C in 5% CO<sub>2</sub>, cells were harvested and cultured in medium with 500 mg/ml G418 (Invitrogen) and 250 mg/ml Hygromycin (Invitrogen). After 14 days, surviving cells were collected, sorted and analyzed using flow cytometry.

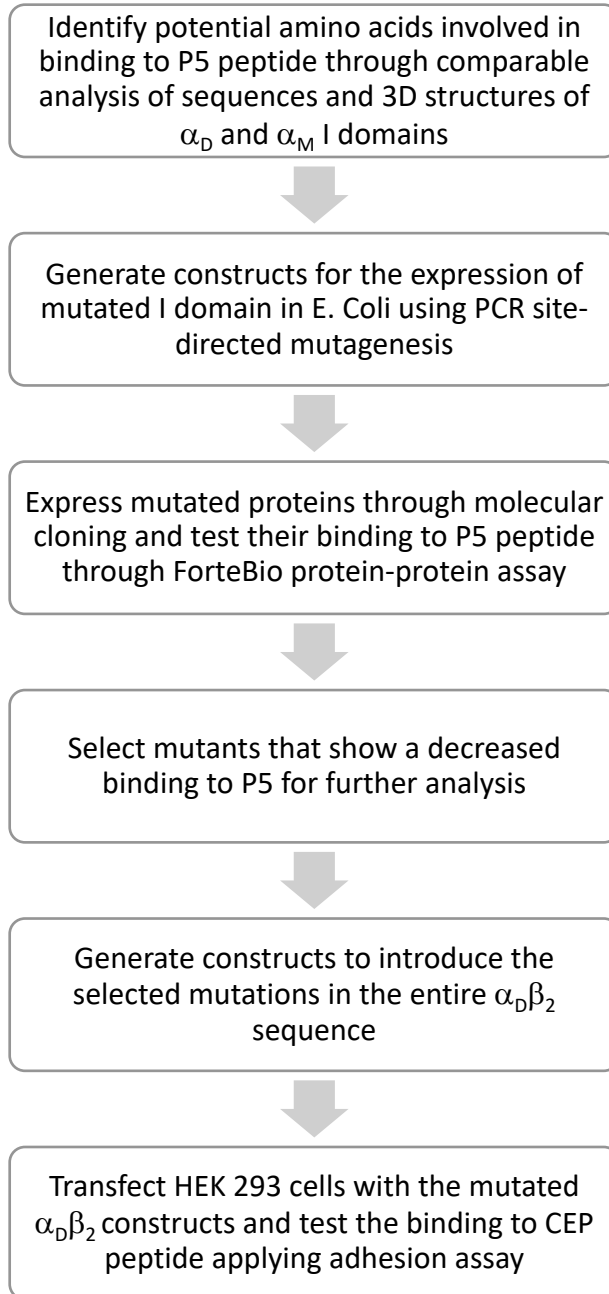
### *Cell Sorting*

FACS analyses were performed to assess the expression of receptors on the surface of the cells transfected with  $\alpha_D\beta_2$  integrin. The cells were incubated with anti- $\alpha_D$  polyclonal Ab and anti- $\beta_2$  mAb IB4 and analyzed using a FACScanä (Beckton Dickinson) as described. The populations of cells expressing similar amounts of  $\alpha_D\beta_2$  and  $\alpha_D\beta_2$  K246 mutant were selected by fluorescence activated cell sorting using a BD Biosciences FACS Vantage Instrument.

### *Cell Adhesion*

For adhesion assays, 96-wells tissue culture plates (Costar, Cambridge, MA) were coated with CEP-BSA and fibrinogen for 3 h at 37°C. The wells were post-coated with 0.5% PVA for 1 h at 22°C to block non-specific binding to the plate. The transfected HEK293 cells in DMEM/F-12 were labeled with 10 mM Calcein AM (Molecular Probes, Eugene, OR) and incubated at 37°C for 30 minutes. The cells were then washed with DMEM/F-12 and then diluted with HBSS to  $1 \times 10^6$ /ml. After washing the plate 3 times with PBS, 50 uL of cells were added to each well, followed by incubation for 30 minutes at 37°C and 5%CO<sub>2</sub>. 200 uL PBS added to each well to wash the cells. Then, the buffer was removed by shaking out and the fluorescent signal on the plate was assessed.

### *Experimental Design Flow Through*



## CHAPTER 3. RESULTS

### *Selection of $\alpha_D$ I-domain Amino Acids for Analysis*

The goal of this project was to identify amino acids of human macrophage integrin  $\alpha_D\beta_2$  which facilitate binding to P5 peptide. Our focus was the  $\alpha_D$  subunit I-domain as this domain is responsible for ligand binding. Because the P5 peptide carries a strong negative charge, we propose that basic amino acid residues of the  $\alpha_D$  I-domain facilitate the binding P5 peptide. To begin compiling a list of  $\alpha_D$  I-domain amino acids potentially involved in the interaction with P5, a comparative analysis using NCBI BLAST was performed comparing the amino acid sequences of  $\alpha_D$  and  $\alpha_M$ . Basic amino acid residues of the  $\alpha_D$  I-domain which are not shared with  $\alpha_M$  were of interest as the P5 peptide does not bind to other closely related members of the integrin family by design, including  $\alpha_M$  which shares around 60% homology. From the  $\alpha_D$ - $\alpha_M$  BLAST analysis, 10 such amino acids were selected for potential analysis as shown in Figure 4.

<b>aD</b>	109	<u>LLGSRW-EIIQTVPDATPECPHQEMDIVFLIDGSGSIDQNDFNQMKGFVQAVMGQFEGTD</u>	167
		L GS + Q P+A CP ++ DI FLIDGSGSI +DF +MK FV VM Q + +	
<b>aM</b>	109	LFGSNLRQQPQKFPEALRGCPQEDSDIAFLIDGSGSII PHDFRRMKEFVSTVMQQLKKS	168
<b>aD</b>	168	<u>TLFALMQYSNLLKIHFTFTQFR</u> <b>RTS</b> PSQQSLVDPIVQL <b>K</b> GLTFTATGILTVVTQLF <b>HHK</b> NG	227
		TLF+LMQYS +IHFTF +F+ +P+ +SLV PI QL G T TATGI VV +LF+ NG	
<b>aM</b>	169	TLFSLMQYSEEFRIHFTFKEFQNNPNRSLVKPITQLLGRTHHTATGIRKVVRELFNITNG	228
<b>aD</b>	228	<u>ARKSA</u> <b>K</b> KILIVITDGQ <b>KY</b> <u>KD</u> PLEYSDVIPQAEKAGIIRYAIGV <b>G</b> HAFQGP <b>TAR</b> QELNTIS	287
		ARK+A KIL+VITDG+K+ DPL Y DVIP+A++ G+IRY IGVG AF+ +RQELNTI+	
<b>aM</b>	229	ARKNAFKILVVITDGEKFGDPLGYEDVIPEADREGVIRYVIGVGDAFRSEKSRQELNTIA	288
<b>aD</b>	288	<u>SAPPQDHVF</u> <b>K</b> VDNFAALGSI <b>Q</b> QLQEKIYAVEGTQSRASSSFQHEMSQEGFSTAL <b>TMD</b> GL	347
		S PP+DHVF+V+NF AL +IQ QL+EKI+A+EGTQ+ +SSSF+HEMSQEGFS A+T +G	
<b>aM</b>	289	SKPPRDHVFQVNNFEALKTIQNQLREKIFAIEGTQTGSSSSFEHEMSQEGFSAAITSN <b>GP</b>	348

**Figure 4. Comparative BLAST analysis.** NCBI Blast analysis comparing amino acid sequences of  $\alpha_D$  I-domain to  $\alpha_M$  I-domain. The  $\alpha_D$  I-domain is underlined. The 10 nonhomologous, basic amino acid residues of  $\alpha_D$  I-domain identified are highlighted in yellow.

Next, a computer model generated by Christopher Ardell (shown in Figure 5) of the  $\alpha_D$  I-domain was used to visualize an approximate location for each of the selected amino acids. Using this model, K180 was selected for potential analysis in addition to the 10 amino acids identified from the BLAST comparison.

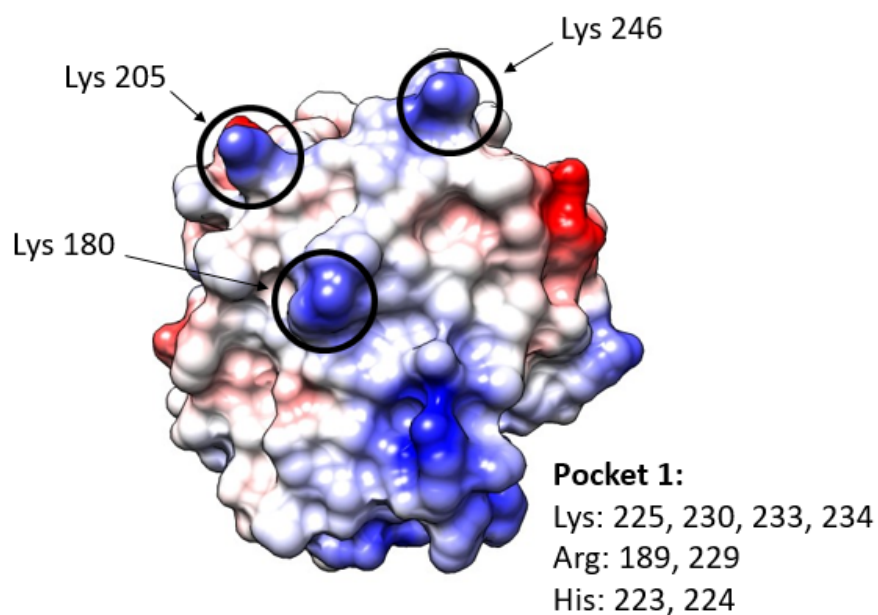


**Figure 5: Predicted Structure of the  $\alpha_D$  I-domain.** Computer generated model of the  $\alpha_D$  I-domain. Areas of positive charge are shown in blue and negative charge is shown in red.

Additionally, the FirstGlance in Jmol software was used to find the location of each corresponding  $\alpha_M$  amino acid for the 10 selected  $\alpha_D$  amino acids. The model for  $\alpha_M$  was generated using PDB identification code 1IDO. The location of each corresponding  $\alpha_M$  amino acid was used to predict the location of the amino acids in  $\alpha_D$ . Amino acids located near the MIDAS site as well as amino acids located on the surface were of great interest. Of the 11 amino acids selected for potential analysis, 9 appeared to have important structural relevance and 8 amino acids were officially selected for mutagenesis: K180, R189, K205, H223, H224, H225, K233, and K246. A summary of this selection process is shown in Table 4 below.



**Table 4: Process of Selecting  $\alpha_D$  I-domain Amino Acids for Mutation.** Amino acids were selected for analysis based on the comparative analysis with  $\alpha_M$  and the structural analysis of the  $\alpha_D$  I domain. Positively charged amino acids are shown in blue, negatively charged amino acids are shown in red.

aD I-domain amino acids selected for potential analysis	Identification Method		Corresponding amino acid in $\alpha_M$	Selected for Analysis
	$\alpha_M$ BLAST	Predicted $\alpha_D$ Structure		
K180	-	✓	R181	✓
R189	✓	✓	Q190	✓
K205	✓	✓	L206	✓
H223	✓	✓	N224	✓
H224	✓	✓	I225	✓
H225	✓	✓	T226	✓
K233	✓	✓	F234	✓
K246	✓	✓	G247	✓
H272	✓	✓	D273	-
K297	✓	-	Q298	-
K309	✓	-	N310	-

The 8 amino acids chosen were subjected to PCR site-directed mutagenesis to create 6 mutant versions of the human  $\alpha_D$  I-domain protein. As amino acids H223, H224, and K225 are located in tandem, they were substituted together to create Mutant HHK223-225[NIT]. The five other chosen amino acids were individually substituted to generate their own mutant I-domains. Each of the selected  $\alpha_D$  amino acids were substituted for the corresponding amino acid in  $\alpha_M$ . In the case that the  $\alpha_M$  amino acid had a bulky side

group or carried a negative charge, the  $\alpha_D$  amino acid was substituted for alanine (A). Mutations to the DNA sequence were carefully chosen using as few DNA base substitutions as possible to create the desired mutation. The DNA primers designed to create the mutation during PCR Site-Directed Mutagenesis were generated using Oligo Software. The amino acid substitution, DNA base substitution and primer sequences used to generate each mutagenic construct are shown below in Table 5.

**Table 5: Generation of Mutant Constructs.** Table 5 shows the amino acid substitutions and DNA base substitutions chosen to generate each of the mutagenic constructs. Additionally, the upper and lower primer sequences designed for PCR-Site Directed Mutagenesis to generate the mutation are listed.

Mutant	Amino Acid Substitution	DNA Base Substitution	Upper Primer Sequence	Lower Primer Sequence
K180	K180 → A180	AAG → GCG	5'- GCAGTACTCAAACCTCCTG GCGATCCATTCACCTCAC C-3'	5'- GGTGAAGGTGAAGTGGATC GCCAGGAGGTTTGAGTACT GC-3'
R189	R189 → Q189	CGG → CAG	5'- CCGTGAACGTCAGGCCTA GCAGTTGGACGATGGG-3'	5'- GGCTCGGGCTGGTCTGGAA TTGGGTGAAGG-3'
K205	K205 → L205	AAA → CTA	5'- CCCATCGTCCAAGTCTAG GCCTGACGTTACAGG-3'	5'- CCGTGAACGTCAGGCCTAG CAGTTGGACGATGGG-3'
HHH223- 225	HHK 223-225 → NIT 223-225	CATCATAAG→ AATATTACG	5'- GGTGACACAGCTATTTAAT ATTACGAATGGGGCCGA AAAAG-3'	5'- CTTTTTCGGGCCCCATTTCGT AATATTAATAGCTGTGTCA CC-3'
K233	K233 → A233	AAG → GCG	5'- GCCCCAAAAAGTGCCGCG AAGATCCTCATTGTC-3'	5'- GACAATGAGGATCTTCGCG GCACTTTTTCGGGC-3'
K246	K246 → A246	AAA → GCA	5'- GATGGGCAGAAGTACGCA GACCCCTGGAATACAG-3'	5'- CTGTATTCCAGGGGGTCTG CGTACTTCTGCCATC-3'

*Mutants K180[A] and R189[Q] are Comparable to Wild-Type I-domain in Binding P5*

Amino acid K180 was selected for analysis despite a basic residue being conserved in  $\alpha_M$  because it was shown to create an area of significant protruding positive charge in the computer-generated model (Figure 5) of the  $\alpha_D$  I-domain near the MIDAS site. The corresponding amino acid in  $\alpha_M$ , R181, is also located in the same area providing more evidence that the predicted location of K180 is correct. We questioned if  $\alpha_D$  amino acid K180 might work together with amino acids K205 and K246, which are located nearby and contribute significant positive charge in a manner similar to K180 as shown in Figure 5.

As the corresponding amino acid in  $\alpha_M$  is also basic, amino acid K180 was substituted for alanine to generate the K180[A] mutant I-domain construct. The construct was sequenced to confirm presence of the K180[A] mutation and then transformed into *E.coli* BL21 cells. The cells were cultured and protein expression was induced by addition of IPTG. The expressed K180[A] I-domain was then isolated using Ni-NTA affinity chromatography. After isolation, the collected protein sample was placed in a 3-step dialysis to change the buffer required for P5 binding testing. Wild-type I-domain also was expressed and isolated in the same manner to later serve as a control in the P5 binding analysis. The K180[A] mutant was expressed and isolated four separate times and binding to P5 was tested for each of the four isolations.

The concentration of isolated Wild-Type and K180[A] I-domain protein was determined by Pierce BCA Assay to be 136 ug/mL and 102.15 ug/mL, respectively. To analyze the purity of protein, a sample of the isolated Wild-Type I-domain and K180[A]

proteins were ran on a 15% acrylamide electrophoresis gel which is shown below in Figure 6.

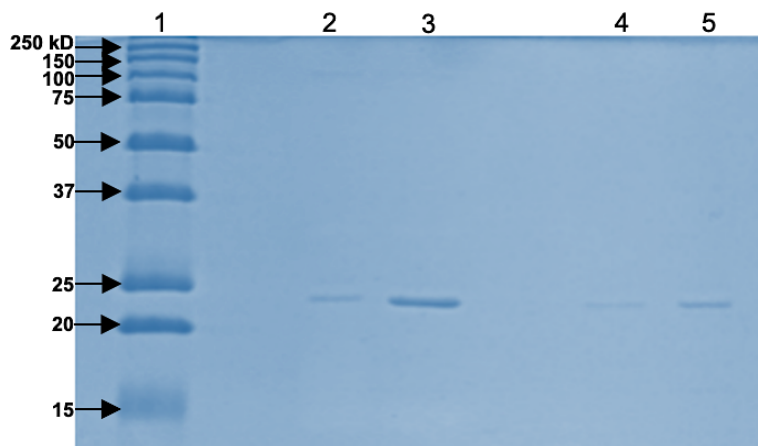


**Figure 6: SDS-polyacrylamide gel electrophoresis (15%) for isolated WT and K180[A] I-domain protein.** Lane 1: Protein Standards. Lane 2: Pre-Dialysis WT I-domain. Lane 3: Post-Dialysis WT I-domain. Lane 4: Pre-Dialysis K180[A] I-domain. Lane 5: Post-Dialysis K180[A] I-domain.

The purified wild-type and K180[A] I-domain proteins were assessed for their ability to bind P5 peptide at two different concentrations, 1.26  $\mu\text{M}$  and 2.5  $\mu\text{M}$  for wild-type and 1.1  $\mu\text{M}$  and 2.21  $\mu\text{M}$  for K180[A], using the ForteBio Octet Protein-Protein assay. Linear biotinylated P5 peptide was immobilized onto a Streptavidin biosensor chip. The ability of wild-type and K180[A] to bind to P5 was measured in real-time by the ForteBio Octet system, as shown in the representative Sensorgram below in Figure 7.

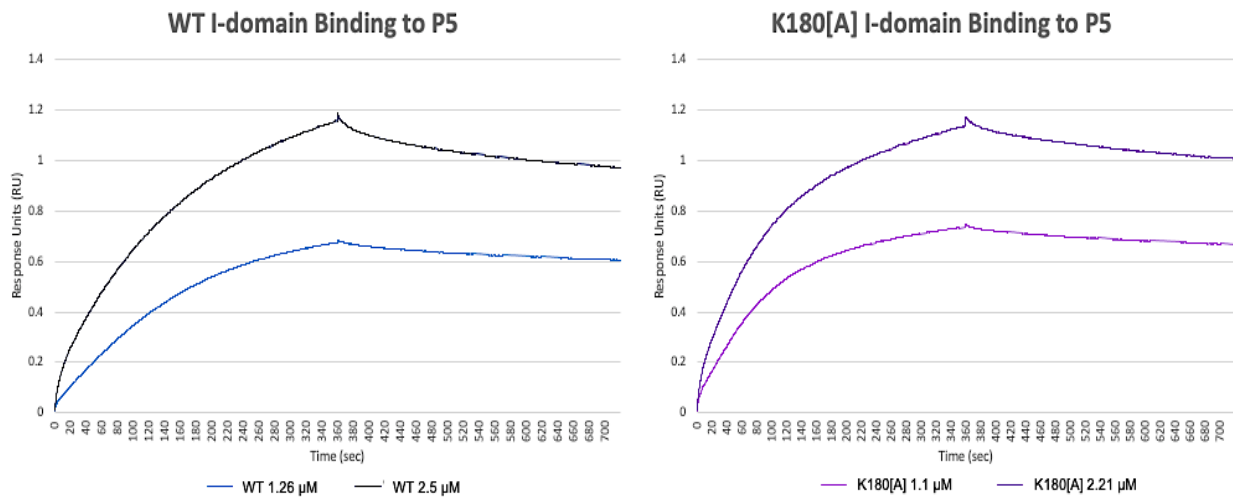


**Figure 7. WT and Mutant K180 I-domain binding to P5.** Representative ForteBio Octet Protein-Protein assay Sensorgram of WT and K180[A] binding to immobilized P5 on a streptavidin biosensor. Association of I-domain binding to P5 occurs from Time 0 to 360 seconds, followed by the dissociation of I-domain from P5 until 700 seconds.

As shown above in Figure 7, the ability of K180[A] to bind P5 peptide was very similar to the Wild-Type  $\alpha_D$  I domain. The shape of the binding curve for both wild-type and K180[A] is rectangular hyperbola and demonstrates non-cooperative, I-domain concentration dependent binding to P5 with moderate affinity. As P5 binding was unaffected by the mutation, amino acid K180 is not involved in the P5 binding interaction.

Amino acid R189 was selected as a basic amino acid is not conserved in this position in  $\alpha_M$ . Additionally, the proposed structure of  $\alpha_D$  shown in Figure 5 places this amino acid as a part of Pocket 1 along with amino acids H223, H224, K225, and K233. Together, these amino acids are believed to form a relatively large area of positive

charge which made each of them of high interest in binding to the negatively charged P5 peptide.

Amino acid R189 was substituted for Glutamine(Q), the corresponding residue in  $\alpha_M$ . The R189[Q] mutant was expressed and isolated two separate times and binding to P5 was tested for each of the two isolated protein samples. The concentrations of protein used in the R189[Q] Sensorgram in Figure 9 were determined using BCA Assay concentrations of 164.9 ug/mL for Wild-Type I-domain and 238.09 ug/mL for the R189[A] mutant. Wild-Type I-domain and R189[Q] proteins was ran on a 15% acrylamide electrophoresis gel which is shown below in Figure 8.

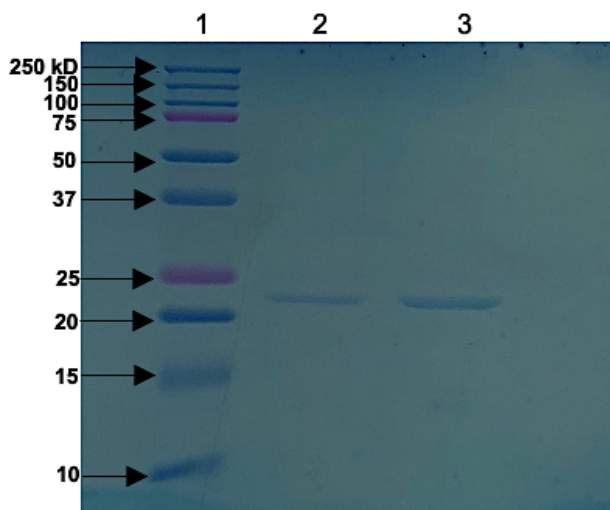


**Figure 8. SDS-polyacrylamide gel electrophoresis (15%) for isolated WT and R189[Q] I-domain protein.** Lane 1: Protein Standards. Lane 2: Post-Dialysis WT I-domain. Lane 3: Post-Dialysis R189[Q] I-domain.

The R189[Q] I-domain protein was tested for its ability to bind P5 peptide compared to Wild-Type I domain by ForteBio Octet Protein-Protein assay. A representative Sensorgram from the ForteBio Octet assay for Wild-Type and mutant R189[Q] I-domains binding to P5 peptide is shown below in Figure 9.

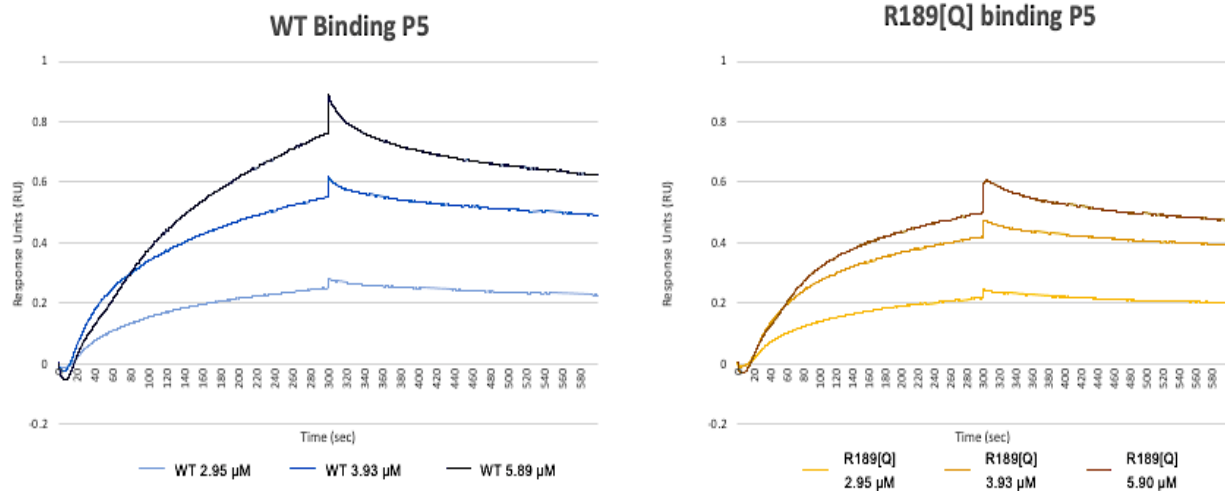


**Figure 9. WT and Mutant R189[Q] I-domain binding to P5.** Representative ForteBio Octet Protein-Protein assay Sensorgram of WT and R189[Q] binding to immobilized P5. I-domain binding to P5 occurs from Time 0 to 360 seconds, followed by the dissociation of I-domain and P5 until 700 seconds.

R189[Q] I-domain demonstrated slightly reduced but similar maximum binding to P5 peptide as compared to the Wild-Type. Sensorgram binding curves demonstrate moderate affinity to P5 and concentration dependent binding for both Wild-Type and R189[Q] mutant. Amino acid R189 is not involved in binding to P5 as only a small difference in binding is observed after mutation.

*Mutants K205[L], HHK223-225[NIT] and K233[A] Demonstrated an Increase in P5 Binding Compared to Wild-Type I-domain*

Amino acid K205 was selected as a basic amino acid residue is not conserved in this position in  $\alpha_M$ . In the proposed structure of the  $\alpha_D$  I-domain shown in Figure 5, amino acid K205 creates an area of significant positive charge protruding from the surface making it of important interest.

The K205 amino acid was substituted for Leucine (L), the corresponding amino acid in  $\alpha_M$ . The K205[L] mutant was expressed and purified two separate times for P5-binding analysis. For ForteBio analysis, the concentration of isolated I-domain protein was confirmed by Pierce BCA Assay to be 108.75 ug/mL for Wild-Type I domain and 119.6 ug/mL for K205[L] I domain. The 15% acrylamide electrophoresis gel shown below in Figure 10 shows the purity of isolated Wild-Type I-domain and K205[L] I domains.

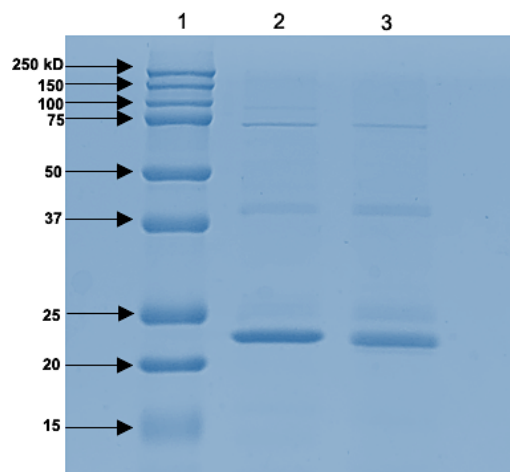


**Figure 10. SDS-polyacrylamide gel electrophoresis (15%) for isolated WT and K205[L] I-domain protein.** Lane 1: Protein Standards. Lane 2: Post-Dialysis WT I-domain. Lane 3: Post-Dialysis K205[L] I-domain.



The isolated wild-type and K205[L] I-domain proteins were assessed for their ability to bind P5 peptide by ForteBio Octet Protein-Protein. A representative Sensorgram from the ForteBio Octet assay testing three different concentrations of wild-type I-domain (1.29  $\mu\text{M}$ , 2.59  $\mu\text{M}$ , and 3.88  $\mu\text{M}$ ) and mutant K205[L] I-domain (1.25  $\mu\text{M}$ , 2.50  $\mu\text{M}$ , and 3.75  $\mu\text{M}$ ) binding to P5 peptide is shown below in Figure 11.

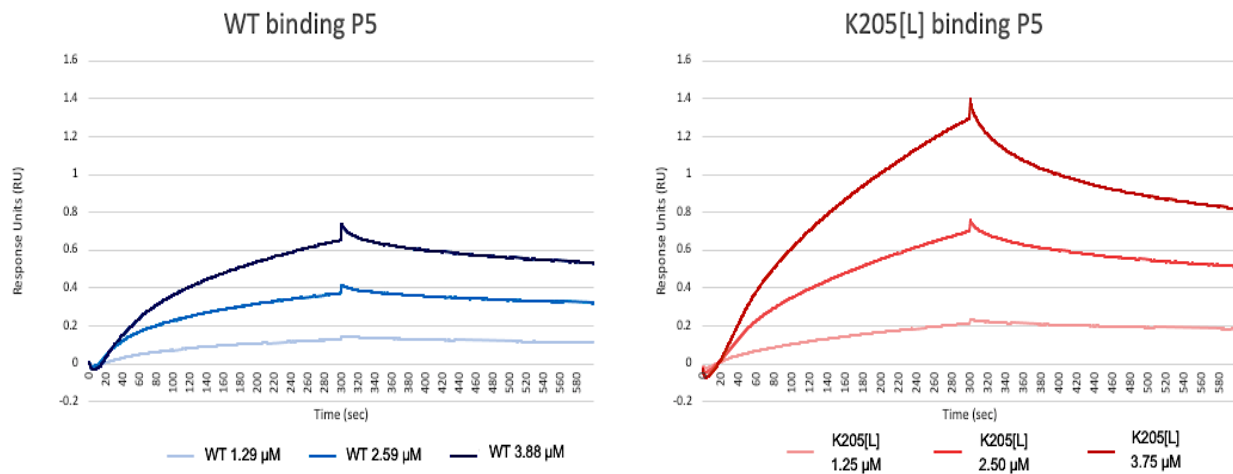


**Figure 11. WT and Mutant K205[L] I-domain binding to P5.** Representative ForteBio Octet Protein-Protein assay Sensorgram of WT and K205[L] binding to P5 peptide on a streptavidin biosensor. Association of I-domain and P5 during occurs from 0 to 300 seconds, followed by the dissociation of I-domain and P5 until 580 seconds.

As shown in Figure 11, K205[L] I-domain demonstrated increased binding to P5 peptide compared to the Wild-Type I-domain. This increased binding can be explained by slight conformational change in the I-domain structure due to the redistribution of surface charge. However, this result clearly demonstrates that amino acid K205 is not involved

in P5 binding to  $\alpha_D$  I-domain, as the K205 substitution to leucine did not cause a decrease in the level of binding observed.

Amino acids H223, H224, and K225 were chosen because a basic amino acid is not conserved in these positions in  $\alpha_M$ . Additionally, these amino acids are believed to form an integral part of Pocket 1, an area of significant positive charge in the  $\alpha_D$  I-domain shown in Figure 5. The role of amino acids composing this positively charged Pocket 1 were of high interest in binding to the negatively charged P5 peptide. As amino acids H223, H224, and K225 are located in tandem, they were substituted for the corresponding residues in  $\alpha_M$ , Asparagine (N), Isoleucine (I), and Threonine (T) respectively to create the HHK223-225[NIT] mutant  $\alpha_D$  I-domain. The ability of the HHK223-225[NIT] mutant I-domain to bind P5 peptide was tested using two separately expressed and purified protein samples. Pierce BCA Assay determined to protein sample concentrations to be 133 ug/mL for Wild-Type I-Domain and 144 ug/mL for HHK223-225[NIT] I-domain. A 15% acrylamide electrophoresis gel containing samples of the isolated Wild-Type and HHK223-225[NIT] I-domain proteins is shown below in Figure 12.

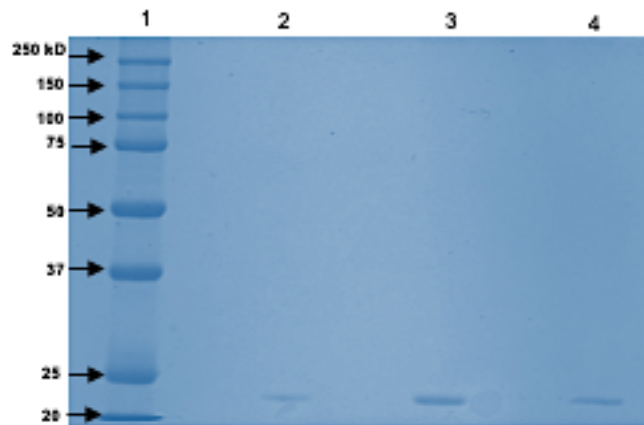


**Figure 12. SDS-polyacrylamide gel electrophoresis (15%) for isolated WT and HHK223-225[NIT] I-domain protein.** Lane 1: Protein Standards. Lane 2: Post-Dialysis WT I-domain. Lane 3: Pre-Dialysis HHK223-225[NIT] I-domain. Lane 4: : Post-Dialysis HHK223-225[NIT] I-domain.

The representative ForteBio sensorgram displaying 4 different concentrations of isolated wild-type I-domain (0  $\mu$ M, 1.58  $\mu$ M, 3.16  $\mu$ M, and 4.75  $\mu$ M) and HHK223-225[NIT] I-domain (0  $\mu$ M, 1.71  $\mu$ M, 3.43  $\mu$ M, and 5.14  $\mu$ M) binding to P5 peptide is shown in Figure 13 below.

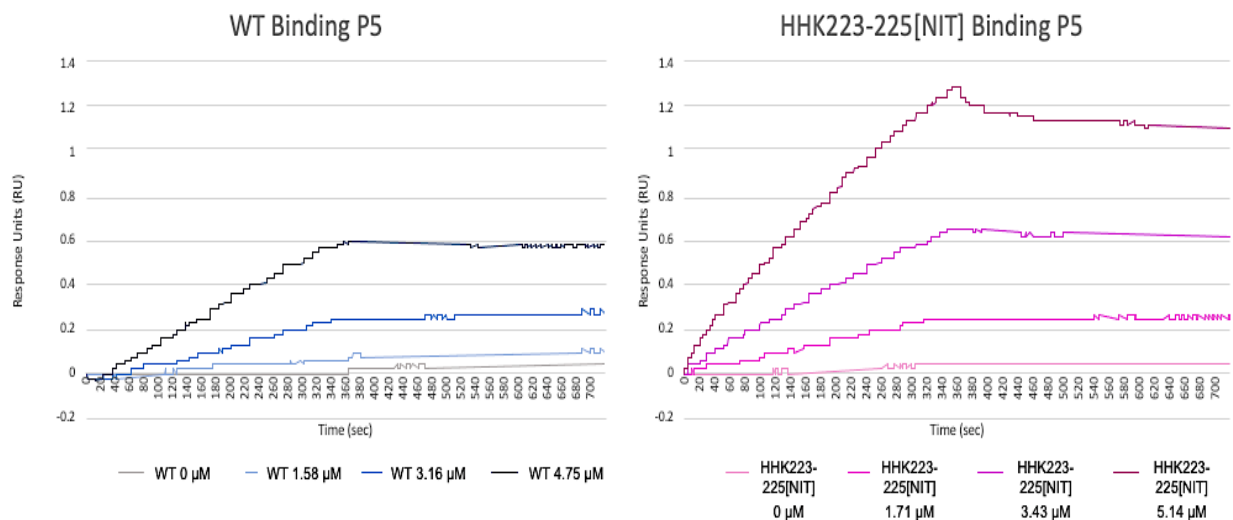


**Figure 13. WT and Mutant HHK223-225[NIT] I-domain binding to P5.** Representative ForteBio Octet Protein-Protein assay Sensorgram of WT and HHK223-225[NIT] I-domain binding to P5. Association of I-domain and P5 peptide begins at time 0 until 360 seconds, followed by the dissociation of I-domain and P5 until 700 seconds.

Interestingly, the HHK223-225[NIT] mutant I-domain demonstrated a significant increase in ability to bind P5 peptide compared to the wild-type I-domain in a concentration dependent manner. The increased binding may be related to some conformational change in I-domain structure. Additionally, the level of binding to P5 for this wild-type I-domain was reduced compared to the typical levels of wild-type binding recorded in tests with other mutants. This implies that a reduced amount of P5 peptide was immobilized onto the streptavidin biosensor. Nevertheless, this result demonstrates that HHK223-225 sequence is not responsible for the binding of  $\alpha_D$  I domain to P5 peptide.

Amino acid K233 was initially selected through comparative analysis of sequences with the  $\alpha_M$  I-domain. Also, the proposed structure of  $\alpha_D$  shown in Figure 5

places this amino acid within Pocket 1, the large region of positively charged amino acids of great interest in potential binding to the negatively charged P5 peptide. Amino acid K233 was substituted for Alanine (A) for expression and isolation two separate times for P5 binding analysis. The concentration of isolated I-domain protein was 153.9 ug/mL for Wild-Type and 215.16 ug/mL for K233[A] as determined by Pierce BCA Assay. The electrophoresis gel containing Wild-Type and K233[A] I-domain protein is shown below in Figure 14.

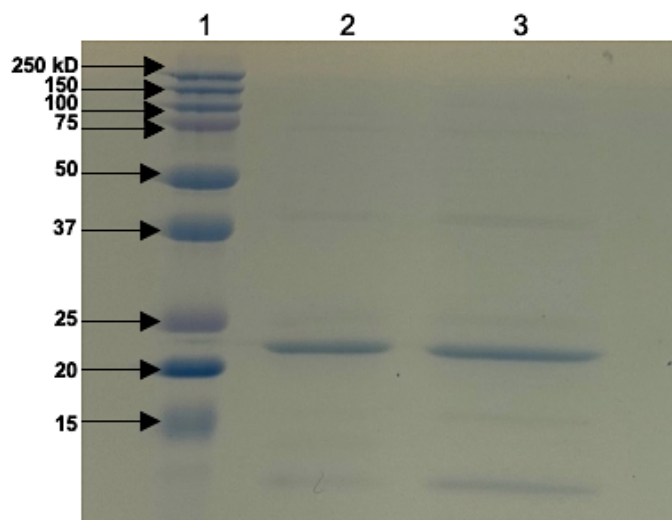


**Figure 14. SDS-polyacrylamide gel electrophoresis (15%) for isolated WT and K233[A] I-domain protein.** Lane 1: Protein Standards. Lane 2: Post-Dialysis WT I-domain. Lane 3: Post-Dialysis K233[A] I-domain.

The isolated wild-type and K223[A] I-domains were analyzed for their ability to bind P5 peptide by ForteBio Octet Protein-Protein assay in the same manner as described for previous mutants. A representative Sensorgram from the ForteBio Octet assay for wild-type and mutant K223[A] I-domain binding to P5 peptide is shown below in Figure 15.

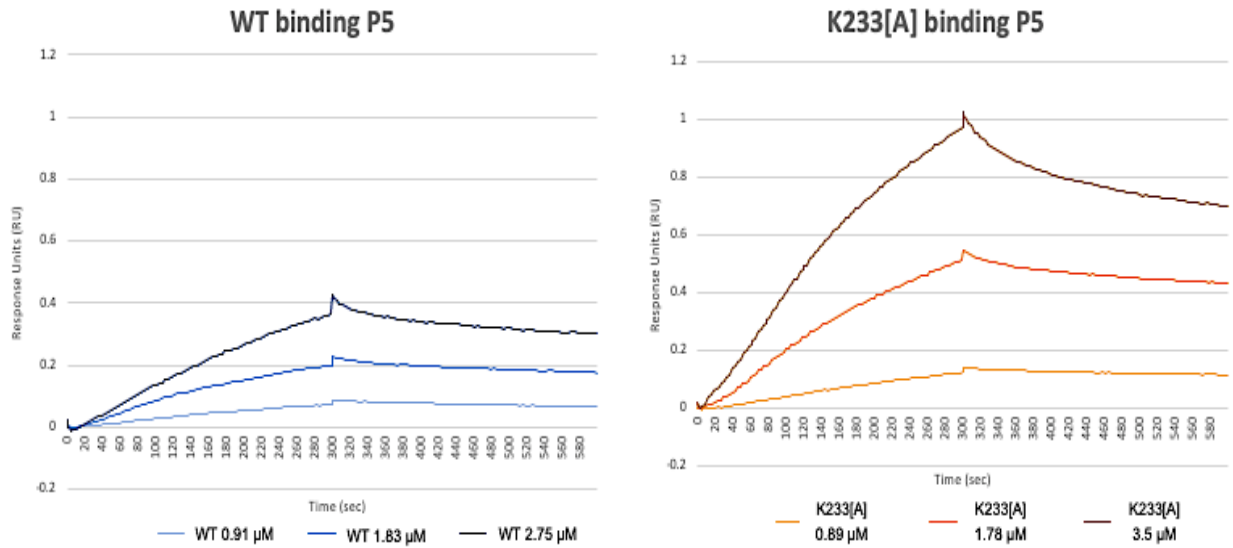


**Figure 15. WT and Mutant K233[A] I-domain binding to P5.** Representative ForteBio Octet Protein-Protein assay Sensorgram of WT and K233[A] binding to immobilized P5. I-domain binding to P5 during Association occurs from Time 0 to 300 seconds, followed by the dissociation of I-domain and P5 until 580 seconds.

The K233[A] mutant I-domain also demonstrated a significant increase in ability to bind P5 peptide compared to the wild-type I-domain in a concentration dependent manner similar to the previously described HHK223-225[NIT] mutant. Both mutants represent substitutions in positively charged Pocket 1 (Fig.5). As we discussed above, we hypothesize that disturbance of this Pocket leads to conformational change which affects binding.

*Mutant K246 Demonstrated a Dramatic Reduction in Binding to both P5 Peptide and CEP Compared to Wild-Type*

Amino acid K246 was selected during the comparative sequence analysis as a basic amino acid is not conserved in this position in  $\alpha_M$ . The proposed structure of  $\alpha_D$  in Figure 6 shows this amino acid contributing a significant area of protruding positive charge near the MIDAS site. Further, a Glycine is conserved in this position in both the  $\alpha_M$  and  $\alpha_X$  integrins which do not bind to P5 peptide. Amino acid K246 was substituted for Alanine (A), and the K246[A] mutant was expressed and isolated four separate times to test binding to P5 peptide. The concentration of isolated I-domain protein was confirmed Pierce BCA Assay, reading 164.917 ug/mL for Wild-Type I-domain and 148.667 ug/mL for K246[A] I-domain. Samples of the isolated Wild-Type and K246[A] I-domain proteins were ran on the SDS-Page on a 15% poly-acrylamide electrophoresis gel shown below in Figure 16.

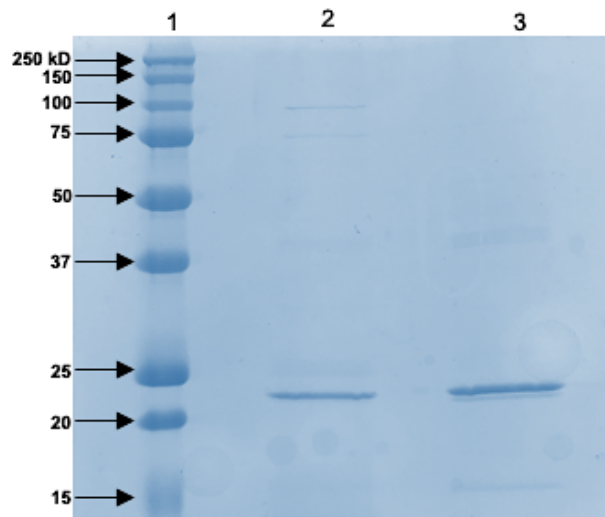


**Figure 16: SDS-polyacrylamide gel electrophoresis (15%) for isolated WT and K246[A] I-domain protein.** Lane 1: Protein Standards. Lane 2: Post-Dialysis WT I-domain. Lane 3: Post-Dialysis K246[A] I-domain.

Four concentrations of wild-type I-domain (0  $\mu\text{M}$ , 1.96  $\mu\text{M}$ , 3.93  $\mu\text{M}$ , and 5.89  $\mu\text{M}$ ) and K246[A] I-domain (0  $\mu\text{M}$ , 1.77  $\mu\text{M}$ , 3.54  $\mu\text{M}$ , and 5.31  $\mu\text{M}$ ) were tested for ability to bind P5 peptide by ForteBio Octet Protein-Protein assay in the same manner as described for previous mutants. A representative Sensorgram from the ForteBio Octet assay for wild-type and Mutant K246[A] I-domain binding to P5 peptide is shown below in Figure 17.

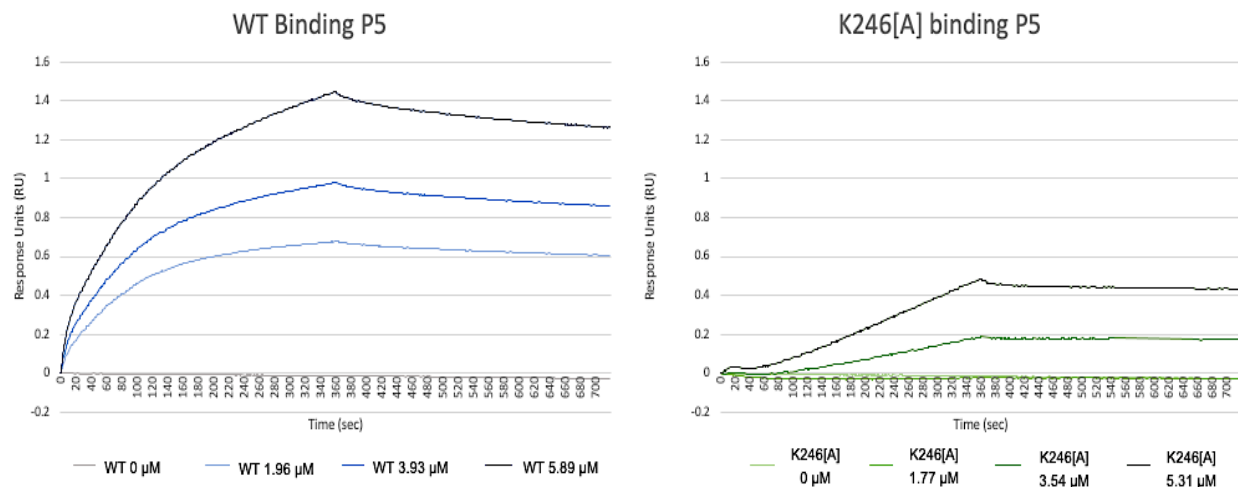


**Figure 17. WT and Mutant K246[A] I-domain binding to P5.** Representative ForteBio Octet Protein-Protein assay Sensorgram of WT and K246[A] binding to immobilized P5 on a streptavidin biosensor. The association of I-domain and P5 peptide occurs from Time 0 to 360 seconds, which is followed by the dissociation of I-domain and P5 until 700 seconds.

As shown in Figure 17, the K246[A] mutant clearly demonstrates a significant reduction in binding to P5 peptide compared to the Wild-Type I-domain. The shape of the binding curve for Wild-Type I-domain is rectangular hyperbola and demonstrates moderate



affinity for P5, while the K246[A] I-domain demonstrated a drastic reduction in binding. Because binding was significantly diminished, we then tested the ability of the K246[A] I-domain to bind to CEP using ForteBio Protein-Protein Assay. CEP was immobilized onto an activated Amine Reactive ARG2 biosensor and I-domain binding to CEP was measured in real time as shown below in Figure 18.

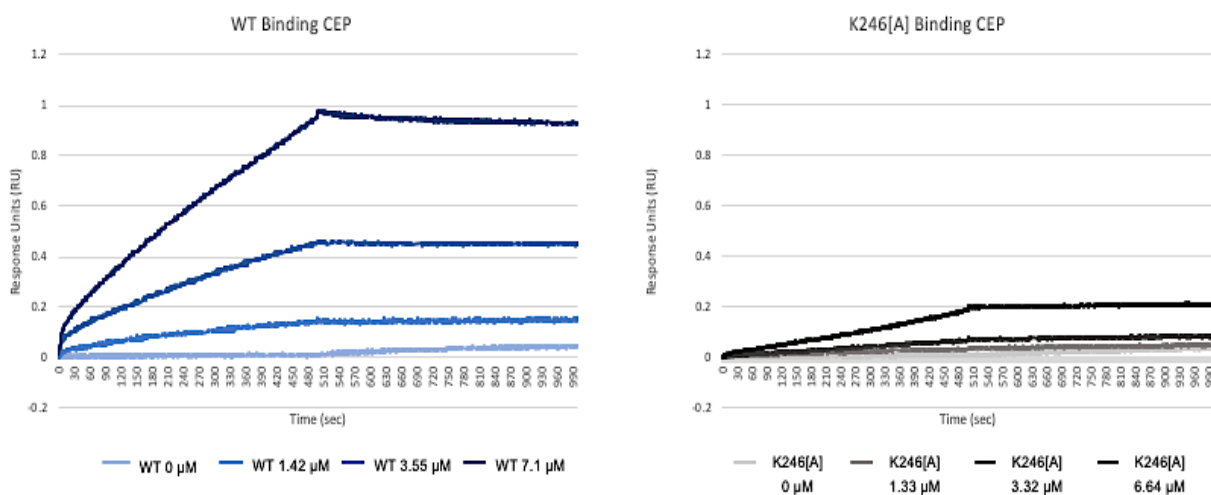


**Figure 18. WT and Mutant K246[A] I-domain binding to CEP.** Representative ForteBio Octet Protein-Protein assay Sensorgram of WT and K246[A] binding to immobilized CEP on an Amine-Reactive Arginine biosensor. The association of I-domain and CEP occurs from Time 0 to 500 seconds, which is followed by the dissociation of I-domain and CEP until 1000 seconds.

K246[A] binding to CEP was tested with ForteBio 3 times, each assay clearly showing that amino acid K246 is involved in binding to CEP as demonstrated by a significant reduction in measured binding.

### Comparison of Wild-Type and Mutant I-domain Binding P5 Peptide

To compare the binding ability of all mutants to P5 peptide, the maximum concentration of each mutant I-domain was converted to a percentage relative to the Wild-Type I-domain binding tested in each assay. The comparison of all mutants reveals that only mutant K246[A] demonstrated a significant, drastic reduction in ability to bind to P5 peptide as shown in Figure 19 below.

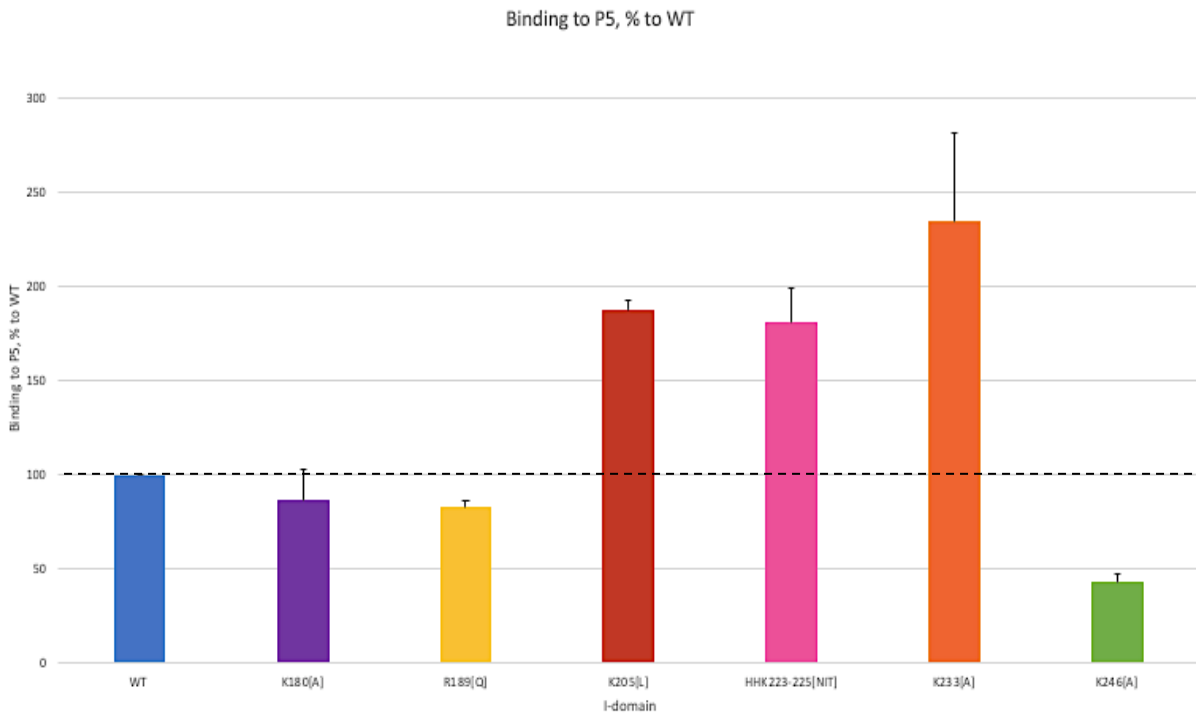


**Figure 19. Comparison of Mutant I-Domains Binding to P5 Peptide.** Mutant I-domains binding to P5 as measured by ForteBio Protein-Protein Assay shown as a percentage to Wild-Type. Wild-Type binding to P5 peptide was calculated as 100% and is represented as the dotted line. N=2 for each mutant I-domain, excluding K180[A] where N=4.

*$\alpha_D\beta_2$ -K246[A] Transfected HEK293 Cells Demonstrated a Significant Reduction in Binding to CEP*

As the K246[A] mutation greatly reduced the I-domain's ability to bind P5 peptide and CEP during the ForteBio assays, we decided to verify our finding using the entire integrin  $\alpha_D\beta_2$  receptor expressed on the surface of HEK293 cells. The cells were tested by adhesion assay to immobilized CEP and also to fibrinogen.

The K246[A] I-domain mutation was introduced into a construct containing the entire integrin  $\alpha_D$  sequence, which was previously cloned in pcDNA3.1 (Neo) vector, using PCR Site-Directed Mutagenesis as described in the Methods. HEK293 cells were transfected with the integrin  $\beta_2$  construct (pcDNA3.1 (hygro) vector) and integrin  $\alpha_D$ -K246[A] mutagenic construct using Lipofectamine 2000. Positive clones were selected after 14 days incubation with 500 ug/ml G418 and 250ug/ml hygromycin. The cells with similar surface density of wild-type  $\alpha_D\beta_2$  and K246[A] mutant were selected by Cell sorting (Fig.21 A).

The ability of Wild-type and K246[A] mutant  $\alpha_D\beta_2$ -transfected HEK293 cells to bind CEP was assessed by cell adhesion assay as described in the methods. Wild-type  $\alpha_D\beta_2$ -transfected HEK293 cells served as the control. The Wild-Type and  $\alpha_D\beta_2$ -K246[A] transfected HEK293 cells adhesion to CEP is shown below in Figure 20 B,C.

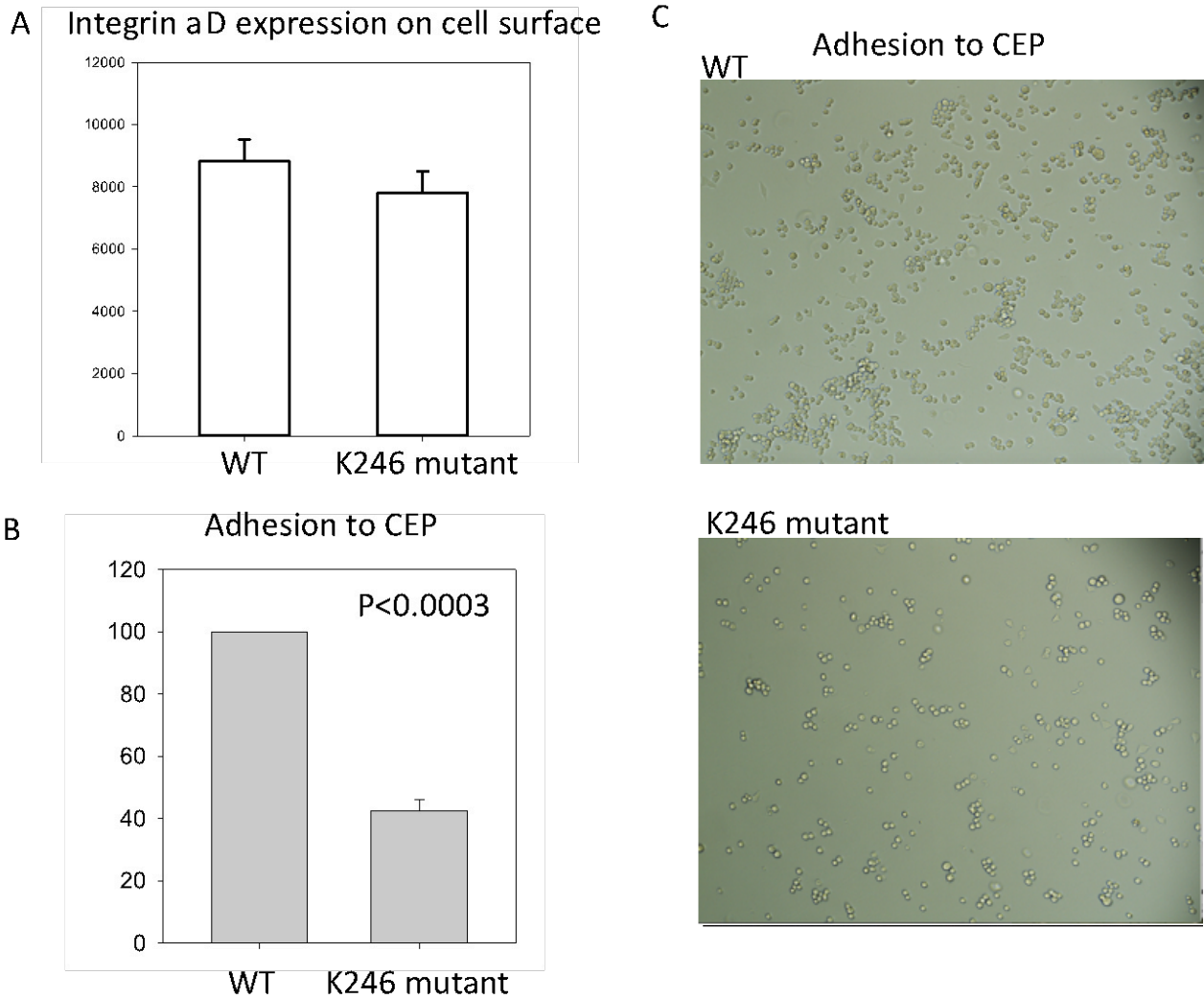


**Figure 20. WT and K246 Mutant  $\alpha_D\beta_2$ -Transfected HEK293 Cells Adhering to CEP.**

Transfected HEK293 Cells containing the K246 mutation showed significant decrease in adhesion to CEP compared to the Wild-Type. A. The level of integrin  $\alpha_D$  expression evaluated by flow cytometry with anti- $\alpha_D$  polyclonal antibody. B. Adhesion of WT and K246 Mutant to CEP calculated as a percent to WT. Representative result from 4 performed experiments. Statistical analysis was calculated using Student's t-test,  $p < 0.003$ . C. Microscopical image of WT and K246 mutant HEK 293 cell adherence to CEP on plate. Magnification 100x.

As described above in Figure 20, adhesion to CEP for transfected HEK293 cells containing the K246[A] mutation was significantly reduced compared to the Wild-Type. This finding indicates that amino acid K246 is likely involved in the integrin  $\alpha_D\beta_2$ -CEP interaction. Adhesion of Wild-Type and K246 mutant  $\alpha_D\beta_2$  cells to fibrinogen was also tested, as fibrinogen is another known ligand of integrin  $\alpha_D\beta_2$ .

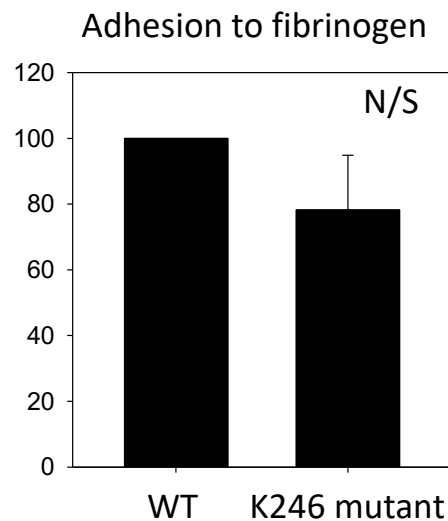


**Figure 21: WT and K246 Mutant  $\alpha_D\beta_2$ -Transfected HEK293 Cells Adhering to Fibrinogen.** Transfected HEK293 Cells containing the K246 mutation showed no significant difference in adhesion to fibrinogen compared to the Wild-Type. Statistical analysis was performed using Student's t-test.

As shown above in Figure 21, there was no significant difference in the ability of K246 Mutant  $\alpha_D\beta_2$ -Transfected HEK293 to bind to fibrinogen compared to the Wild-type. Importantly, this finding confirms that the K246 mutant integrin is stable and capable of binding ligand in a manner similar to the Wild-Type  $\alpha_D\beta_2$  integrin – providing more evidence that amino acid K246 is involved in binding to the P5 peptide and CEP.

## CHAPTER 4. DISCUSSION

Integrin  $\alpha_D\beta_2$  has been shown to promote macrophage retention and accumulation within inflamed tissue, a key event in development of chronic inflammation. The upregulation of integrin  $\alpha_D\beta_2$  on pro-inflammatory macrophages is believed to function as a brake signal which prevents further migration after arrival at the site of inflammation. However, during chronic inflammatory reactions this macrophage accumulation and retention within inflamed tissue leads to host tissue damage, formation of chronic inflammatory lesion, and eventually development of chronic inflammatory disease.

Because of the unique upregulation of integrin  $\alpha_D\beta_2$  on inflammatory macrophages, it is an attractive target to prevent chronic inflammation. After identifying 2-( $\omega$ -carboxyethyl) pyrrole (CEP), an oxidative modification to proteins and phospholipids found within inflamed tissue, as a ligand for integrin  $\alpha_D\beta_2$ , a specific inhibitor targeting the integrin  $\alpha_D\beta_2$ -CEP interaction was created. The resulting 15 amino acid peptide, called P5, successfully reduced macrophage retention and accumulation within inflamed tissue both *in vitro* and *in vivo*. The purpose of this thesis was to identify amino acids of human macrophage integrin  $\alpha_D\beta_2$  which participate in binding to P5 peptide and likewise to CEP.

As the P5 peptide carries a strong negative charge and does not bind to other similar integrins by design, we hypothesized that basic amino acid residues of the  $\alpha_D$  subunit I-domain which are not conserved among members of the  $\beta_2$  integrin family are responsible for binding to P5. Through comparative analysis of sequences and structures, 8 amino acids of the  $\alpha_D$  subunit I-domain were selected to create 6 mutant I-

domains for analysis: K180[A], R189[Q], K205[L], HHK223-225[NIT], K233[A], and K246[A].

Though the location and protruding positive charge generated by  $\alpha_D$  amino acid K180 seemed to play a role in binding to P5, this amino acid is likely not involved in the P5- $\alpha_D\beta_2$  or CEP- $\alpha_D\beta_2$  interaction as no difference in binding was observed compared to the Wild-Type I-domain. As a basic residue is conserved in this position in the  $\alpha_M$  subunit, R181, perhaps  $\alpha_D$  amino acid K180 participates in binding fibrinogen or other ligands also recognized by the  $\alpha_M$  subunit.

Mutation of  $\alpha_D$  amino acid R189 lead to a slight decrease in binding to P5 peptide as measured by ForteBio but overall there was not a significant difference as compared to Wild-Type I-domain. As this amino acid is located in Pocket 1 of the  $\alpha_D$  subunit, the slight decrease in binding could point to an important role in ligand binding for this pocket. However, the other amino acids within this pocket which were analyzed, HHK223-225[NIT] and K233[A], displayed a significant increase in binding. We hypothesize that disruptions to Pocket 1 lead to a redistribution of surface charge which exposes additional ligand binding sites and results in the observed increased in binding.

Interestingly, mutant K205[L] also demonstrated a significant increase in binding to P5 compared to the Wild-Type I-domain as measured by ForteBio Protein-Protein Assay. The potential explanation for this increase in binding is also related to changes in the 3D conformation of the I-domain, leading to exposition of additional ligand binding sites which are naturally unavailable. Nevertheless, these findings show that these amino acids are not involved in binding to P5 peptide.

Of the 6 mutant  $\alpha_D$  I-domains analyzed, only one mutant, K246[A], showed a dramatic and significant reduction in ability to bind to both P5 peptide and CEP as measured by ForteBio. Further, adhesion to CEP was also significantly reduced compared to the Wild-Type when the K246[A] mutation was introduced into the entire integrin  $\alpha_D\beta_2$  receptor and expressed on the surface of HEK293 cells. Adhesion to fibrinogen for cells expressing the  $\alpha_D\beta_2$ -K246[A] mutant showed no effect compared to the Wild-Type, indicating that the mutant I-domain is conformationally stable and is not critical for the binding to fibrinogen.

Despite several key functions in inflammation, pathogen response, and tissue injury, much remains unknown about integrin  $\alpha_D\beta_2$ . These findings are important because they provide more detail into ligand recognition and binding for this understudied integrin. Future directions include a continuation of this study focused on identifying the other amino acids involved in the  $\alpha_D\beta_2$ -CEP interaction, as this is the first step in developing a major therapeutic antibody with potential to prevent chronic inflammation. Antibody targeting  $\alpha_D$  amino acids which bind to CEP, including amino acid K246 identified in this study, would prevent macrophage adherence within sites of inflammation and effectively reduce macrophage accumulation and retention within inflamed tissue, thus reducing or eliminating chronic inflammatory reactions. As chronic inflammation affects millions of people around the globe, we hope these findings serve as a stepping stone in the future development of a clinically relevant inhibitor of chronic inflammation.



## REFERENCES

1. Freire MO, Dyke TEV. Natural resolution of inflammation. *Periodontology* 2000. 2013;63(1):149-164. doi:10.1111/prd.12034.
2. Chen L, Deng H, Cui H, et al. Inflammatory responses and inflammation-associated diseases in organs. *Oncotarget*. 2017;9(6):7204-7218. Published 2017 Dec 14. doi:10.18632/oncotarget.23208
3. Sugimoto MA, Sousa LP, Pinho V, Perretti M and Teixeira MM (2016) Resolution of Inflammation: What Controls Its Onset? *Front. Immunol.*7:160. doi: 10.3389/fimmu.2016.00160
4. Pahwa R, Goyal A, Bansal P, et al. Chronic Inflammation. [Updated 2020 Aug 10]. In: *StatPearls* [Internet]. Treasure Island (FL): StatPearls Publishing; 2020 Jan-. Available from: <https://www.ncbi.nlm.nih.gov/books/NBK493173/>
5. Furman D, Campisi J, Verdin E, et al. Chronic inflammation in the etiology of disease across the life span. *Nat Med*. 2019;25(12):1822-1832. doi:10.1038/s41591-019-0675-0
6. Irving D. Chronic Conditions in America: Price and Prevalence. *Rand Review*. 2017. Available from: <https://www.rand.org/blog/rand-review/2017/07/chronic-conditions-in-america-price-and-prevalence.html>
7. Ponzoni M, Pastorino F, Di Paolo D, Perri P, Brignole C. Targeting Macrophages as a Potential Therapeutic Intervention: Impact on Inflammatory Diseases and Cancer. *Int J Mol Sci*. 2018;19(7):1953. Published 2018 Jul 4. doi:10.3390/ijms19071953
8. Davignon JL, Hayder M, Baron M, et al. Targeting monocytes/macrophages in the treatment of rheumatoid arthritis. *Rheumatology (Oxford)*. 2013;52(4):590-598. doi:10.1093/rheumatology/kes304
9. Punchard, N. A., Whelan, C. J., & Adcock, I. (2004). The Journal of Inflammation. *Journal of inflammation (London, England)*, 1(1), 1. doi:10.1186/1476-9255-1-1
10. Sutton N.R., Baek A., Pinsky D.J. (2014) Endothelial Cells and Inflammation. In: Mackay I.R., Rose N.R., Diamond B., Davidson A. (eds) *Encyclopedia of Medical Immunology*. Springer, New York, NY. [https://doi.org/10.1007/978-0-387-84828-0\\_184](https://doi.org/10.1007/978-0-387-84828-0_184)
11. Voisin MB, Nourshargh S. Neutrophil transmigration: emergence of an adhesive cascade within venular walls. *J Innate Immun*. 2013;5(4):336-347. doi:10.1159/000346659
12. Selders GS, Fetz AE, Radic MZ, Bowlin GL. An overview of the role of neutrophils in innate immunity, inflammation and host-biomaterial integration. *Regen Biomater*. 2017;4(1):55-68. doi:10.1093/rb/rbw041
13. Prame Kumar K, Nicholls AJ, Wong CHY. Partners in crime: neutrophils and monocytes/macrophages in inflammation and disease. *Cell Tissue Res*. 2018;371(3):551-565. doi:10.1007/s00441-017-2753-2
14. Oishi Y, Manabe I. Macrophages in inflammation, repair and regeneration. *International Immunology*, 2018;30(11)511–528. doi.org/10.1093/intimm/dxy054

15. Das A, Sinha M, Datta S, et al. Monocyte and macrophage plasticity in tissue repair and regeneration. *Am J Pathol.* 2015;185(10):2596-2606. doi:10.1016/j.ajpath.2015.06.001
16. Parisi L, Gini E, Baci D, Tremolati M, Fanuli M, Bassani B, Farronato G, Bruno A, Mortara L. Macrophage Polarization in Chronic Inflammatory Diseases: Killers or Builders? *Journal of immunology research.* 2018;2018(8917804). doi:10.1155/2018/8917804
17. Atri C, Guerfali FZ, Laouini D. Role of Human Macrophage Polarization in Inflammation during Infectious Diseases. *Int J Mol Sci.* 2018;19(6):1801. Published 2018 Jun 19. doi:10.3390/ijms19061801
18. Italiani P, Boraschi D. From Monocytes to M1/M2 Macrophages: Phenotypical vs. Functional Differentiation. *Front Immunol.* 2014;5(514). doi:10.3389/fimmu.2014.00514.
19. Krzyszczyk P, Schloss R, Palmer A, Berthiaume F. The Role of Macrophages in Acute and Chronic Wound Healing and Interventions to Promote Pro-wound Healing Phenotypes. *Front Physiol.* 2018;9:419. Published 2018 May 1. doi:10.3389/fphys.2018.00419
20. Tabas I, Glass CK. Anti-inflammatory therapy in chronic disease: challenges and opportunities. *Science.* 2013;339(6116):166-172. doi:10.1126/science.1230720
21. Nathan C, Ding A. Nonresolving inflammation. *Cell.* 2010 Mar 19;140(6):871-82. doi:10.1016/j.cell.2010.02.029. PMID: 20303877.
22. Murray PJ, Wynn TA. Protective and pathogenic functions of macrophage subsets. *Nat Rev Immunol.* 2011;11(11):723-737. Published 2011 Oct 14. doi:10.1038/nri3073
23. Weiss U. Inflammation. *Nature.* 2008;454(427). <https://doi.org/10.1038/454427a>
24. Hynes RO. Integrins: A Family of Cell Surface Receptors. *Cell.* 1987;48(4):549-554. [https://doi.org/10.1016/0092-8674\(87\)90233-9](https://doi.org/10.1016/0092-8674(87)90233-9)
25. Zhang K, Chen J. The regulation of integrin function by divalent cations. *Cell Adh Migr.* 2012;6(1):20-29. doi:10.4161/cam.18702
26. Campbell ID, Humphries MJ. Integrin structure, activation, and interactions. *Cold Spring Harb Perspect Biol.* 2011;3(3):a004994. Published 2011 Mar 1. doi:10.1101/cshperspect.a004994
27. Hynes RO. Integrins: bidirectional, allosteric signaling machines. *Cell.* 2002 Sep 20;110(6):673-87. doi:10.1016/s0092-8674(02)00971-6. PMID: 12297042.
28. Takada Y, Ye X, Simon S. The integrins. *Genome Biol.* 2007;8(5):215. doi:10.1186/gb-2007-8-5-215
29. Pan L, Zhao Y, Yuan Z, Qin G. Research advances on structure and biological functions of integrins. *SpringerPlus.* 2016;5(1094).
30. Barczyk M., Carracedo S. & Gullberg D. Integrins. *Cell Tissue Res.* 2010; 339(269). <https://doi.org/10.1007/s00441-009-0834-6>
31. Gahmberg CG, Fagerholm SC, Nurmi SM, Chavakis T, Marchesan A, Gronholm M. Regulation of Integrin Activity and Signaling. *BBA.* 2009;1790(6):431-444. <https://doi.org/10.1016/j.bbagen.2009.03.007>
32. Larson RS, Corbi AL, Berman L, Springer T. Primary structure of the leukocyte function-associated molecule-1 alpha subunit: an integrin with an embedded domain

- defining a protein superfamily. *J Cell Biol.* 1989 Feb;108(2):703-12. doi: 10.1083/jcb.108.2.703. PMID: 2537322; PMCID: PMC2115430.
33. Brown KL, Banerjee S, Feigley A. et al. Salt-bridge modulates differential calcium-mediated ligand binding to integrin  $\alpha$ 1- and  $\alpha$ 2-I domains. *Sci Rep.* 2018; 8(2916). <https://doi.org/10.1038/s41598-018-21231-1>--Pan L, Zhao Y, Yuan Z, Qin G. Research advances on structure and biological functions of integrins. *SpringerPlus.* 2016;5(1094).
  34. Fagerholm SC, Guenther C, Lloret Asens M, Savinko T, Uotila LM. Beta2-Integrins and Interacting Proteins in Leukocyte Trafficking, Immune Suppression, and Immunodeficiency Disease. *Front Immunol.* 2019;10:254. Published 2019 Feb 19. doi:10.3389/fimmu.2019.00254
  35. Arnaout MA. Biology and structure of leukocyte  $\beta$  2 integrins and their role in inflammation. *F1000Res.* 2016;5:F1000 Faculty Rev-2433. Published 2016 Oct 4. doi:10.12688/f1000research.9415.1
  36. Beta2 integrins. *Rheumatology and Immunology Therapy.* Springer, Berlin, Heidelberg. 2004. doi.org/10.1007/3-540-29662-X\_435
  37. Van der Viren M, Trong HL, Wood CL, Moore PF, St. John T, Staunton DE, Gallatin WM. A Novel Leukointegrin  $\alpha$ D $\beta$ 2, Binds Preferentially to ICAM-3. *Immunity.* 1995;3:683-690.
  38. Harris ES, McIntyre TM, Prescott SM, Zimmerman GA. The Leukocyte Integrins. *Journal of Biol Chem.* 2000; 275: 23409-23412. doi: 10.1074/jbc.R000004200
  39. Miyazaki Y, Vieira-de-Abreu A, Harris ES, Shah AM, Weyrich AS, Castro-Faria-Neto HC, Zimmerman GA. Integrin  $\alpha$ D $\beta$ 2 (CD11d/CD18) is expressed by human circulating and tissue myeloid leukocytes and mediates inflammatory signaling. *PLoS One.* 2014 Nov 21;9(11):e112770. doi: 10.1371/journal.pone.0112770. PMID: 25415295; PMCID: PMC4240710.
  40. Schittenhelm L, Hilkens CM, Morrison V. B2 Integrins as Regulators of Dendritic Cell, Monocyte, and Macrophage Function. *Front. Immunol.* 2017; 8:1866. doi: 10.3389/fimmu.2017.01866
  41. Salomon RG, Hong L, Hollyfield JG. Discovery of carboxyethylpyrroles (CEPs): critical insights into AMD, autism, cancer, and wound healing from basic research on the chemistry of oxidized phospholipids. *Chem Res Toxicol.* 2011;24(11):1803-1816. doi:10.1021/tx200206v
  42. Witztum JL. CEP Is an Important and Ubiquitous Oxidation Specific Epitope Recognized by Innate Pattern Recognition Receptors. *Circ Res.* 2015;117(4):305-308. doi:10.1161/CIRCRESAHA.115.306928
  43. Yakubenko VP, Cui K, Ardell CL, et al. Oxidative modifications of extracellular matrix promote the second wave of inflammation via  $\beta$ 2 integrins. *Blood.* 2018;132(1):78-88. doi:10.1182/blood-2017-10-810176
  44. Aziz MH, Cui K, Das M, et al. The Upregulation of Integrin  $\alpha$ D $\beta$ 2 (CD11d/CD18) on Inflammatory Macrophages Promotes Macrophage Retention in Vascular Lesions and Development of Atherosclerosis. *J Immunol.* 2017;198(12):4855-4867. doi:10.4049/jimmunol.1602175
  45. Yakubenko VP, Belevych N, Mishchuk D, Schurin A, Lam SC, Ugarova TP. The role of integrin alpha D beta2 (CD11d/CD18) in monocyte/macrophage migration. *Exp Cell Res.* 2008;314(14):2569-2578. doi:10.1016/j.yexcr.2008.05.016

46. Cui K, Podolnikova NP, Bailey W, Szmuc E, Podrez EA, Byzova TV, Yakubenko VP. Inhibition of integrin  $\alpha$ D $\beta$ 2-mediated macrophage adhesion to end product of docosahexaenoic acid (DHA) oxidation prevents macrophage accumulation during inflammation. *J Biol Chem.* 2019;294(39):14370-14382. doi: 10.1074/jbc.RA119.009590.

VITA  
CADY FORGEY

Education: M.S. Biology, East Tennessee State University, Department  
of Biomedical Sciences, Johnson City, Tennessee,  
2020  
B.A. Health Sciences, East Tennessee State University,  
Johnson City, Tennessee, 2017

Professional Experience: Graduate Assistant, East Tennessee State University,  
College of Arts and Sciences, 2018-2020  
Research Assistant, East Tennessee State University,  
College of Arts and Sciences, 2018-2020

Honors and Awards: William Harvey Fraley and Nina M. Fraley Memorial  
Research Award, East Tennessee State University,  
2020